Leaf trait acclimation amplifies simulated climate warming in response to elevated carbon dioxide

Marlies Kovenock[1] and Abigail L. S. Swann[2,1]

[1] Department of Biology, University of Washington, Seattle, WA, USA
[2] Department of Atmospheric Sciences, University of Washington, Seattle, USA

Correspondence to: M. Kovenock, kovenock@uw.edu

Supporting Information S1

Accepted by *Global Biogeochemical Cycles* on July 31, 2018
https://doi.org/10.1029/2018GB005883

Abstract

Vegetation modifies Earth's climate by controlling the fluxes of energy, carbon, and water. Of critical importance is a better understanding of how vegetation responses to climate change will feedback on climate. Observations show that plant traits respond to elevated carbon dioxide concentrations. These plant trait acclimations can alter leaf area and, thus, productivity and surface energy fluxes. Yet the climate impacts of plant structural trait acclimations remain to be tested and quantified. Here we show that one leaf trait acclimation in response to elevated carbon dioxide – a one-third increase in leaf mass per area – significantly impacts climate and carbon cycling in Earth system model experiments. Global net primary productivity decreases (-5.8 PgC/year, 95% confidence interval [$CI_{95\%}$] -5.5 to -6.0), representing a decreased carbon dioxide sink of similar magnitude to current annual fossil fuel emissions (8 PgC/year). Additional anomalous terrestrial warming (+0.3 °C globally, $CI_{95\%}$ 0.2 to 0.4), especially of the northern extratropics (+0.4 °C, $CI_{95\%}$ 0.2 to 0.5), results from reduced evapotranspiration and enhanced absorption of solar radiation at the surface. Leaf trait acclimation drives declines in productivity and evapotranspiration by reducing leaf area growth in response to elevated carbon dioxide, as a one-third increase in leaf mass per area raises the cost of building leaf area and productivity fails to fully compensate. Our results suggest that plant trait acclimations, such as changing leaf mass per area, should be considered in climate projections and provide additional motivation for ecological and physiological experiments that determine plant responses to environment.

Plain Language Summary

Plants have been observed to change their traits, such as the thickness of leaves, in response to future environmental conditions, but the implications of these changes for climate have not yet been quantified. We show that changes in plant traits could have large-scale climate impacts, including higher temperatures and relative decreases in plant photosynthesis which have not been previously accounted for. Our findings suggest an urgent need for observations of how plant traits will respond to future environmental conditions as well as a need for a better understanding of the underlying mechanisms so that they can be included in climate projections.

Key Points

- Acclimation of leaf traits to elevated CO_2 significantly altered global climate and carbon cycling in Earth system model experiments
- Higher carbon cost of building leaf area under elevated CO_2 offsets gains in leaf area, productivity, and evapotranspiration
- Results identify an urgent need to collect observations to constrain uncertainty in plant trait responses to a changing climate

Keywords

global warming, vegetation feedbacks, plant traits, carbon cycle, climate impact

1. Introduction

Feedbacks between vegetation and climate change are of critical importance to future climate projections but remain highly uncertain (Arora et al., 2013; Friedlingstein et al., 2014; Lovenduski & Bonan, 2017; Pu & Dickinson, 2012). Vegetation strongly influences the Earth's climate by controlling the fluxes of carbon, water, and energy between the land surface and the atmosphere (Bonan, 2008). Changes in biologically mediated carbon fluxes, such as productivity and respiration, can alter the concentration of carbon dioxide (CO_2) in the atmosphere, leading to warming of the Earth due to the radiative effects of CO_2. Given that these radiative effects are driven by biological sources of carbon, we refer to the associated temperature increase as biogeochemical warming. Since the start of the industrial era, Earth's vegetation has removed about 30% of anthropogenic CO_2 emissions from the atmosphere (Ciais et al., 2013). Changes in vegetation can also induce warming by altering water and energy fluxes through their influence on Earth surface properties such as evapotranspiration, albedo, and roughness. We refer to increases in temperature due to alterations of the surface energy balance as biogeophysical warming. Transpiration, the biologically controlled flux of water from soil through plants into the atmosphere, makes up an estimated 60% of current terrestrial water fluxes (Wei et al., 2017), which physically cool the land surface. Rising CO_2 concentrations are expected to have profound and wide reaching effects on vegetation functioning and growth, with important implications for global carbon uptake and evapotranspirative cooling. Yet large uncertainty exists in the magnitude, and even the sign, of vegetation feedbacks on climate change (Arora et al., 2013; Friedlingstein et al., 2014; Lovenduski & Bonan, 2017; Pu & Dickinson, 2012). This uncertainty stems in large part from the challenge of representing complex and diverse life-forms at the global scale in the Earth system models used to project future climate (Lovenduski & Bonan, 2017). Key biological processes must be missing or poorly constrained, but we lack a clear understanding of which processes are essential for predicting climate and carbon cycling changes.

Incorporating observations of plant trait distributions and their responses to environmental drivers into Earth system models is proposed as a way to improve predictions of ecosystem functioning (Butler et al., 2017; Fisher et al., 2015; Kattge & Knorr, 2007; Kattge et al., 2011; Pavlick et al., 2013; Reich et al., 2014; Reichstein et al., 2014; Scheiter et al., 2013; Van Bodegom et al., 2012; Verheijen et al., 2015, 2013; Wright et al., 2004). Trait databases and studies that aggregate observations across species are beginning to make it possible to characterize current plant trait distributions and their responses to environmental drivers at the global scale (e.g., Kattge et al., 2011; Kattge & Knorr, 2007; Niinemets, 2001; Van Bodegom et al., 2012; Verheijen et al., 2013; Wright et al., 2004). However, the biogeographic relationship between traits and climate across ecosystems, caused primarily by environmental filtering, does not tell us about short-term responses to changes in climate within an ecosystem, caused by

acclimation (Van Bodegom et al., 2012; Verheijen et al., 2013). The climate impacts of these two distinct responses, environmental filtering and acclimation, have been tested in previous work.

Studies focused on environmental filtering have shown that allowing traits to vary temporally based on observed spatial relationships between these traits and environmental drivers (i.e., space-for-time substitution) has carbon uptake and climate implications (Verheijen et al., 2013, 2015). This approach estimates the integrated outcome of numerous biological responses to climate (e.g., adaptation, changes in species distribution, and acclimation; Van Bodegom et al., 2012; Verheijen et al., 2015). However, it does not separate the impacts of individual biological responses (e.g., acclimation, adaptation, and species turnover) from one another and therefore cannot mechanistically explain the underlying causes of trait variation (Verheijen et al., 2013). Further, it is uncertain if space-for-time relationships used in the environmental filtering approach will hold under future climate in part because acclimation of traits may alter these trait-environment relationships (Fisher et al., 2015; Verheijen et al., 2015). Acclimation responses can differ in magnitude and even direction from trait responses to environmental filtering (e.g., Poorter et al., 2009; Verheijen et al., 2013).

Other studies have directly investigated the influence of some trait acclimations to temperature and elevated CO_2 (e.g., photosynthetic and stomatal conductance rates) and found profound effects on large-scale climate and carbon cycling (Betts et al., 1997; Cao et al., 2010; Lombardozzi et al., 2015; Pu & Dickinson, 2012; Sellers et al., 1996; Smith et al., 2017). Acclimation occurs within the same individual plant and on short-time scales (e.g., a growing season), making it immediately relevant for 21st century climate. Prior studies have focused on rate traits and have not considered the potential climate feedbacks of plant structural traits. Trait responses to climate change that alter plant structure could feedback on climate and carbon cycling by modifying the surface areas (e.g., leaf area) over which the rates of photosynthesis and stomatal conductance are summed.

Among the most widely observed plant structural trait responses to elevated CO_2 is an increase in leaf mass per area (g leaf carbon/m^2 leaf area). Leaf mass per area represents the carbon cost of building leaf area and is a quantity commonly used in Earth system models to convert from carbon available for leaf growth to leaf area. Field and greenhouse manipulation experiments show that leaf mass per area increases by as much as one third in response to elevated CO_2 in a wide range of C_3 plants, including trees, shrubs, and crops, across a variety of ecosystems on many continents (Ainsworth & Long, 2005; Medlyn et al., 1999, 2015; Poorter et al., 2009). Acclimation to warming temperatures could potentially offset leaf mass per area increases due to elevated CO_2 but is limited to cold regions such as the boreal and arctic (Poorter et al., 2009). Most Earth system models project increases in leaf area in response to CO_2 over the 21st century (Mahowald et al., 2016; Swann et al., 2016), which are expected to negatively feedback on climate change by promoting carbon uptake from the atmosphere and evapotranspirative cooling over land (Betts et al., 1997; Bounoua et al., 2010; Pu & Dickinson, 2012). However, few models capture the decreased sensitivity of leaf area index to increases in

leaf biomass at elevated CO_2 because they fail to represent the concomitant increase in leaf mass per area (De Kauwe et al., 2014; Medlyn et al., 2015).

Here we quantify the potential extent of climate and carbon cycling impacts of leaf mass per area acclimation to rising CO_2 using a series of Community Earth System Model coupled atmosphere-land-carbon cycle simulations (supporting information Table S1). In the model, vegetation responds to climate by changing carbon assimilation, stomatal conductance, biomass, and leaf area. These vegetation responses can induce biogeophysical warming through feedbacks on the surface energy balance and atmosphere via changes in albedo, evapotranspiration, and surface roughness. We quantify the additional climate impacts, beyond those of elevated CO_2, of leaf mass per area acclimation to CO_2 as the difference between a leaf acclimation experiment and a climate change control simulation (CCLMA-CC). As atmospheric CO_2 concentration is held invariant over time in all simulations, biogeochemical warming is estimated from the difference in net primary productivity. The level of leaf acclimation, a one-third increase in leaf mass per area in C_3 plants, was estimated from the upper bound of acclimation to a doubling of CO_2 (355 to 710 ppm) from Poorter et al.'s (2009) meta-analysis of approximately 200 studies, which provides the most plant-type-specific CO_2 acclimation relationships for leaf mass per area currently available. The control simulation (CTRL) provides a reference for whether the effects of leaf acclimation at elevated CO_2 (CCLMA-CC) moderate (e.g., reduce the increase in leaf area) or enhance (e.g., further increase leaf area) changes due to elevated CO_2 alone (CC-CTRL). We also estimate the effects of leaf mass per area acclimation to temperature (TCCLMA-CC) and the historical influence of changing leaf mass per area (LMA-CTRL). Maximum photosynthetic rates (e.g., V_{cmax25} and J_{max25}) are the same across these simulations (CCLMA, CC, CTRL, TCCLMA, and LMA) before acclimating to temperature following Kattge and Knorr (2007). We test the sensitivity of our results to increasing maximum photosynthetic rates concurrently with leaf mass per area (CCLMAPS).

2. Materials and Methods

This study used the Community Earth System Model version 1.3beta11 with interactive land and biogeochemistry (CLM4.5-BGC; Oleson et al., 2013), atmosphere (CAM5; Neale et al., 2012), mixed-layer ocean (Neale et al., 2012), and sea ice (CICE4; Hunke & Lipscomb, 2010) models. Simulations that couple the land and atmosphere, such as performed here, are required to quantify the climate impacts of changes in the land surface, as they capture the atmospheric response and land-atmosphere feedbacks. To allow for ocean heat transport and atmosphere-ocean interaction while retaining computational economy, we used a mixed-layer ocean model with prescribed lateral heat fluxes rather than a more computationally expensive full dynamical ocean model. We ran the simulations with a spatial resolution of approximately 1.9° by 2.5° gridcells. The biogeochemistry model represents a full terrestrial carbon cycle with growth, mortality, and decay – and hence leaf area and carbon storage in aboveground and belowground pools. The distribution of 15 plant functional types was prescribed by a map of present day

vegetation and held invariable; however, under unsuitable growing conditions, plants diminish to a minimum leaf area.

The climate change control simulation (CC; 2xCO_2, no leaf acclimation) represents the mean climate state when atmospheric CO_2 is fixed at 710 ppm. The CO_2 leaf acclimation experiment (CCLMA; 2xCO_2, +1/3 leaf mass per area) is identical to the climate change control simulation (CC) except that it includes a plausible extent of leaf mass per area acclimation to CO_2 in all C_3 plants (Poorter et al., 2009). (See Text S1.2 for details.) A second experiment (TCCLMA; 2xCO_2, no change in leaf mass per area in boreal and arctic biomes, +1/3 leaf mass per area in all other C_3 plants) tests the impact of leaf acclimation to both CO_2 and temperature (Poorter et al., 2009). (See Texts S1.3 and S2.1 for further details.) Leaf mass per area acclimation to CO_2 and temperature were estimated using the most plant-type-specific acclimation relationships currently available (Poorter et al., 2009). A third experiment (CCLMAPS; 2xCO_2, +1/3 leaf mass per area, +1/3 maximum photosynthetic rates) tests the sensitivity of our results to increasing maximum photosynthetic rates and quantifies the increase in maximum photosynthetic rates required to offset the biogeophysical warming due CO_2 acclimation of leaf mass per area. All elevated CO_2 simulations (CC, CCLMA, TCCLMA, and CCLMAPS) include the effects of CO_2 radiative forcing, CO_2 fertilization, and gains in water use efficiency. A fourth experiment (LMA; 1xCO_2, +1/3 leaf mass per area) tests the sensitivity of historical climate to increased leaf mass per area. A separate control simulation (CTRL; 1xCO_2, no leaf acclimation) represents the equilibrium climate state when CO_2 concentration is fixed at 355 ppm, a common baseline for Earth system model simulations.

We held maximum photosynthetic rates (V_{cmax25}, J_{max25}, and T_{p25}) constant, so that they did not differ between the control (CC and CTRL) and CCLMA, TCCLMA, and LMA simulations prior to temperature acclimation. As the default model calculates maximum photosynthetic rates from leaf mass per area, we modified this relationship so that these rates did not differ (except CCLMAPS). In our simulations a decrease in leaf nitrogen concentration, which can also be thought of as an increase in leaf carbon-to-nitrogen ratio (gC/gN) and a reduction in leaf nutrition, is coupled to the increase in leaf mass per area (except CCLMAPS) to maintain maximum photosynthetic rates at control (CTRL and CC) levels. (See Text S1.2 for details.) This represents a conservative estimate of acclimation of maximum photosynthetic rates to CO_2, as evidence supports a decrease in these rates in response to elevated CO_2 (Ainsworth & Long, 2005; Leakey et al., 2012; Rogers et al., 2017; Smith & Dukes, 2013). The decrease in leaf nitrogen concentration with elevated CO_2 is also supported by observations (reviewed in Ainsworth & Long, 2005; Leakey et al., 2012; Way et al., 2015). All simulations include temperature acclimation of maximum photosynthetic rates (Kattge & Knorr, 2007; Oleson et al., 2013). The maximum photosynthetic rate values of all simulations were within the observed range used to generate the empirical temperature acclimation function, and acclimation was not allowed outside of the range of temperature values used to generate the empirical function.

All simulations were integrated for 85 years, except the CCLMAPS experiment was integrated for 44 years. All experiment simulations were initiated by branching from the

beginning of year 56 of the control run (CTRL). Temperature, leaf area index, net and gross primary productivity, evapotranspiration and live carbon pools (leaf, live stem, live root, and fine root) reached equilibrium before year 30 in each simulation. The first 30 years of each simulation were discarded to allow for spin up. The remaining years were used in our analysis and represent many samples of the equilibrium state. Model results are available through the University of Washington Libraries ResearchWorks digital repository. The URL for the data in the ResearchWorks system is https://digital.lib.washington.edu/researchworks/handle/1773/41856.

We use annual mean changes in biogeophysical warming and net primary productivity to quantify the upper bound of the potential climate and carbon cycling influences of leaf mass per area acclimation. We tested for differences between simulations in the annual mean at the global, latitude band, zonal mean (average for a given latitude), and gridcell scales using bootstrap methods (n = 50,000; Text S1.4) with model years as the unit of replication. Spatial relationships between variables at the gridcell scale were tested using simple, multiple, and stepwise linear regression methods on annual mean values. Differences and relationships were considered significant at the 95% level. (See Text S1.4 for details.) Latitude bands were defined as southern extratropics (60°S to 20°S), tropics (20°S to 20°N), northern extratropics (20°N to 65°N), and northern high latitudes (65°N to 90°N).

Biogeochemical warming was calculated by converting the change in net primary productivity to a change in atmospheric CO_2 level (2 PgC to 1 ppm). After accounting for compensatory carbon uptake by the ocean of 60-85% (Archer et al., 2009; Broecker et al., 1979), we converted the change in atmospheric CO_2 concentration to a radiative forcing in watt per square meter following the methods of Hansen et al. (1998) and Myhre et al. (1998). The resulting global temperature change was then estimated from the forcing using a range of climate sensitivities (temperature change due to a doubling of CO_2) from 1.5 to 4.5 °C.

3. Results

3.1 Biogeophysical Warming

Acclimation of leaf mass per area to elevated CO_2 induced significant biogeophysical warming in addition to the warming caused by the radiative effects of a doubling of CO_2 in Earth system model experiments. The change in temperature from the direct effects of a doubling of CO_2 (from 355 to 710 ppm) in our model (CC-CTRL) was 5.0 °C (95% confidence interval [$CI_{95\%}$] 5.0 to 5.1), with a higher mean warming over land of 6.1 °C ($CI_{95\%}$ 6.0 to 6.1). The influence of doubling CO_2 included plant responses such as carbon fertilization (Oleson et al., 2013) and increased water use efficiency (+27% for CC-CTRL, $CI_{95\%}$ 27 to 28) but did not account for acclimation of leaf mass per area. Consideration of leaf mass per area acclimation to CO_2 (CCLMA-CC) increased annual mean temperature over land by an additional +0.3 °C ($CI_{95\%}$ 0.2 to 0.4, Figure 1a and Tables 1 and S2) and +0.2 °C ($CI_{95\%}$ 0.1 to 0.2) globally on top of the direct effects of CO_2. This acclimation-driven warming was especially pronounced over land in the northern extratropics (+0.4 °C, $CI_{95\%}$ 0.2 to 0.5) due to above average warming over

Eurasia (Figures 1a and 2a and Table 1). The influence of temperature acclimation of leaf mass per area (TCCLMA-CC) was limited to cold biomes and did not significantly alter the amount of additional warming over land and globally due to CO_2 acclimation (Text S2.1; Figure S1). The influence of leaf mass per area changes at historical CO_2 levels (LMA-CTRL) was also small (Text S2.2).

Leaf trait acclimation enhanced biogeophysical warming over land under future CO_2 levels by offsetting the CO_2-induced increase in leaf area index (m^2 leaf area/m^2 ground). Doubling of CO_2 (CC-CTRL) increased the annual mean leaf area index by 1.2 m^2/m^2 ($CI_{95\%}$ 1.2 to 1.2) in our simulations. This magnitude of change is at the high end of Coupled Model Intercomparison Project Phase 5 model leaf area responses to RCP8.5 over the 21st century (Mahowald et al., 2016). Inclusion of leaf mass per area acclimation strongly limited the increase in leaf area index to 0.3 m^2/m^2 ($CI_{95\%}$ 0.2 to 0.3) over the ambient CO_2 simulation (CCLMA-CTRL). This attenuation of leaf area growth occurred in almost all vegetated areas (Figures 1b and 2b and Table 1). However, leaf area index decreased more in response to leaf acclimation in places with high initial leaf areas, as shown by the negative spatial relationship ($r = -0.91$, $R^2 = 0.83$, Figure S2a) between leaf area index in the control climate change case (CC) and the change in leaf area index in response to leaf acclimation (CCLMA-CC).

The reduced increase in leaf area in response to leaf trait acclimation (CCLMA-CC) induced biogeophysical warming over land by shifting the balance between surface energy budget terms. Near-surface temperature warmed in response to a moderation of the increase in evapotranspirative cooling and an increase in solar radiation absorbed at the Earth's surface (Figures 2 and 3c and Tables 1 and S2). These two factors shifted additional energy to sensible heat, the term in the surface energy balance that directly drives surface temperature changes. In the tropics, warming was primarily the result of reduced evapotranspiration, followed by greater solar radiation absorbed at the surface (Figures 2c and 2d and Tables 1 and S2). In the extratropics, increased absorption of solar radiation and reduced evapotranspiration induced warming in more equal proportion (Figures 2b and 2c and Tables 1 and S2). The strong influence on the surface energy budget of evapotranspiration in the tropics and the combination of evapotranspiration and solar radiation in the midlatitudes is consistent with previous studies (Bonan, 2008).

Evapotranspiration is the combination of several contributing water fluxes. Reduced transpiration (CCLMA-CC) represented the largest contribution to evapotranspiration declines in all regions, followed by lower evaporation from leaf surfaces (Tables 1 and S2). However, greater soil evaporation partially offset the decline from transpiration and leaf evaporation. The reduced increase in leaf area index in response to leaf acclimation drove the reduction in evapotranspiration (Figure 2), aided by a slight increase in water use efficiency (CCLMA-CC; +0.5%, $CI_{95\%}$ 0.2 to 0.8). Reductions in evapotranspiration were spatially positively related to changes in leaf area (CCLMA-CC; $r = 0.57$, $R^2 = 0.32$; Figure S2b). As leaf area provides the surface area over which transpiration and leaf evaporation occur, the acclimation-induced reduction of leaf area index diminished evapotranspiration to drive biogeophysical warming.

More solar radiation reached land when leaf mass per area acclimation was included (Figures 2d and 3c and Table 1) due to reduced low cloud cover over the tropics and northern extratropics (Figure S3a). Acclimation-driven warming decreased the relative humidity of the lower atmosphere in these regions (Figure S3b), making it less likely for water vapor to saturate the air and condense to form clouds. Relative humidity decreased because warming of the atmosphere (Figure S3c) raised the saturation vapor pressure, outcompeting the influence of greater absolute amounts of water vapor (i.e., specific humidity) in some areas (Figure S3d). The overall increase in solar radiation at the surface demonstrates that the effect of reduced cloud cover overwhelmed the opposing influence of a small surface albedo increase. Albedo increased because the reduced increase in leaf area index (CCLMA-CC) allowed more radiation to reach and reflect away from bare ground which is brighter than vegetation (Bonan, 2008; Oleson et al., 2013). Albedo changes (Figure S4) were measured by comparing the difference in solar radiation absorbed at the surface under clear-sky conditions (a model calculation that ignores the influence of clouds).

3.2 Carbon Cycle and Biogeochemical Warming

In addition to biogeophysical warming, acclimation of leaf mass per area reduced carbon uptake by the biosphere (Figures 1c and 3c), which would induce further warming by increasing atmospheric CO_2 levels. Net primary productivity increased 51% (+30.1 PgC/year, $CI_{95\%}$ 29.8 to 30.4) in response to a doubling of CO_2 (CC-CTRL). Acclimation of leaf mass per area strongly moderated the positive effect of carbon fertilization on net primary productivity in response to elevated CO_2, reducing the gain in productivity by -5.8 PgC/year (CCLMA-CC; $CI_{95\%}$ -5.5 to -6.0, Tables 1 and S2). This decrease in net primary productivity in response to leaf acclimation was driven by declines in the tropics, followed by the northern extratropics (Tables 1 and S2).

Smaller increases in leaf area and higher temperatures in response to leaf acclimation both contributed to the reduced gains in productivity relative to the climate change control. Decreases in gross primary productivity (CCLMA-CC) were best described by a multiple regression using both changes (CCLMA-CC) in temperature and leaf area as predictors (multiple regression $R^2 = 0.32$; Figure S2d). Changes in net primary productivity were weakly but best related to temperature change ($r = -0.49$, $R^2 = 0.24$; Figure S2c).

From the reduced gains in carbon uptake in response to leaf mass per area acclimation we estimate a change in global mean temperature. Our simulations did not directly account for this biogeochemical warming, as atmospheric CO_2 levels within each simulation were held fixed in time. Instead, we estimate biogeochemical warming (see section 2) associated with the net change in carbon storage from the difference in carbon uptake by vegetation, as measured by net primary productivity, when leaf acclimation is considered (CCLMA-CC). The -5.5 to -6.0-PgC/year reduction in net primary productivity gains would increase global atmospheric CO_2 concentration by +0.4 to +1.2 ppm/year when considering the effect of oceanic buffering. We estimate that this additional atmospheric CO_2 induces biogeochemical warming of +0.1 to +1.0 °C over 100 years, the approximate average time scale for a doubling of CO_2 from 355 to 710

ppm under the Intergovernmental Panel on Climate Change RCP8.5 and RCP6 emissions scenarios (Cubasch et al., 2013). The sum of this biogeochemical warming and the biogeophysical warming reported above brings the total additional warming over land due to leaf mass per area acclimation (CCLMA-CC) to +0.3 to +1.4 °C greater than the warming due to a doubling of CO_2 in the control climate change simulation.

4. Discussion

We find that leaf trait responses could have significant large-scale climate implications. Increased leaf mass per area enhances warming beyond the direct effects of elevated CO_2 by moderating evapotranspiration and enhancing absorption of solar radiation and by lessening the rise in leaf area which lowers net primary productivity gains (Figure 3).

The surface temperature change in response to leaf trait acclimation is of comparable magnitude to the climate response to other important climate forcings (Figure 4). For example, the enhanced warming in our experiment (+0.3 to +1.4 °C) is smaller but of the same order of magnitude as the change in temperature in response to a doubling of CO_2 estimated by the Intergovernmental Panel on Climate Change (+1.5 to +4.5 °C) from observed 20th century climate change, paleoclimate, feedback analysis, and climate models (Ciais et al., 2013). While these comparisons are not exact, as the methods and measures of uncertainty differ, they provide an order of magnitude comparison for our results. Enhanced warming in our experiment is also of greater or comparable magnitude to the temperature response to large-scale land cover change (Figure 4d), such as anthropogenic land cover change over the 20th century (-0.04 °C physical, +0.27 chemical, +0.22 total, over land; Pongratz et al., 2010) and theoretical global deforestation (-1.1 °C biogeophysical over land; Davin & de Noblet-Ducoudré, 2010).

Furthermore, our results show that the surface temperature change in response to leaf trait acclimation can exceed or match several well-studied plant physiological feedbacks to elevated CO_2 that are included in most climate projections (Figure 4c). These include the vegetation carbon-concentration feedback (0 to -1.0 °C; estimated from the change in CO_2 implemented in this study of 355 to 710 ppm and the Coupled Model Intercomparison Project Phase 5 model range for land carbon-concentration feedback parameter from Arora et al., 2013); stomatal conductance response to elevated CO_2 (+0.2 to +0.5 °C biogeophysical over land; Betts et al., 1997, 2007; Boucher et al., 2009; Cao et al., 2010; Cox et al., 1999; Pu & Dickinson, 2012; Sellers et al., 1996); photosynthetic down-regulation (-0.1 to +0.3 °C biogeophysical over land; Bounoua et al., 2010; Pu & Dickinson, 2012); and increased leaf area index (+30 to 60%) due to CO_2 fertilization and increased water use efficiency under elevated CO_2 (-0.1 to -0.4 °C biogeophysical over land; Betts et al., 1997; Bounoua et al., 2010; Pu & Dickinson, 2012).

The reduced increase in terrestrial productivity in response to leaf mass per area acclimation is on the order of other large-scale carbon cycle perturbations and moderates the effect of CO_2 fertilization on plant growth and carbon uptake from the atmosphere. The -5.8-PgC/year ($CI_{95\%}$ -5.5 to -6.0) reduction in net primary productivity in response to leaf mass per

area acclimation in our simulations (CCLMA-CC) is a reduced carbon sink comparable in magnitude to current global fossil fuel emissions (8 PgC/year; Ciais et al., 2013). It is larger than the total current terrestrial biosphere uptake of CO_2 from the atmosphere (3 PgC/year; Le Quéré et al., 2016).

Leaf mass per area acclimation to CO_2 represents a shift in the relationship between two key ecosystem properties – productivity and leaf area. As such, this acclimation will remain important for climate and carbon cycling if other trait responses further modify estimates of productivity. Notably, the magnitude of maximum photosynthetic rate (e.g., V_{cmax25} and J_{max25}) acclimation to CO_2 remains uncertain and difficult to represent at the global scale (Rogers et al., 2017; Smith & Dukes, 2013). While most estimates suggest that maximum photosynthetic rates will decrease in response to CO_2 (Ainsworth & Long, 2005; Leakey et al., 2012; Rogers et al., 2017; Smith & Dukes, 2013), which would amplify our results, we conservatively do not change these rates in our primary experiment (CCLMA-CC). We note that our results should be considered in relation to our treatment of maximum photosynthetic rates, which were equivalent across experiments prior to temperature acclimation in all simulations except CCLMAPS. The CCLMAPS experiment tests the sensitivity of our results to increasing maximum photosynthetic rates. Using this experiment (CCLMAPS-CC), we estimate that maximum photosynthetic rates would need to increase (opposite direction of expected CO_2 acclimation) by one third to bolster net primary productivity enough to offset the biogeophysical warming over land due to leaf acclimation in our experiments (Text S2.3; CCLMAPS-CC). This altered balance between productivity (biogeochemical warming) and leaf area (biogeophysical warming) demonstrates the importance of including leaf mass per area acclimation to CO_2.

In addition to leaf mass per area, other changes in coordinated leaf traits could be expected to occur under climate change and further influence biogeophysical and biogeochemical warming. Longer leaf lifespans are correlated with higher leaf mass per area across species (Wright et al., 2004) and could be expected to offset the climate influence of leaf mass per area by enhancing productivity beyond current estimates. However, this correlation observed across species does not necessarily hold for trait changes within a species, such as in response to acclimation (Anderegg et al., 2018; Fisher et al., 2015; Lusk et al., 2008). Observations of leaf lifespan acclimation to elevated CO_2 indicate that the response is highly variable in magnitude and sign and inconsistently associated with higher leaf mass per area (e.g., Norby et al., 2003, 2010; Taylor et al., 2008, and references therein). As the observational evidence does not support an increase in leaf lifespan in coordination with leaf mass per area acclimation to CO_2, we chose not to impose this change in our simulations. However, we do include changes in leaf area duration due to phenological responses to warming temperature and soil moisture in all simulations (Oleson et al., 2013). Litter decomposition has also been hypothesized to slow with leaf responses to elevated CO_2 with implications for carbon cycling (Strain & Bazzaz, 1983). However, a meta-analysis of observations found that the effect of elevated CO_2 on leaf decomposition processes was not significant, despite changes in leaf litter traits (Norby et al., 2001). We therefore do not test changes in litter decomposition here. Lastly,

changes in leaf nitrogen concentration and anatomy in response to climate change could alter albedo through their influence on leaf reflectance and transmittance (e.g., Ollinger, 2011), a possible avenue for future research. Leaf acclimation in our simulations was allowed to influence albedo indirectly by altering leaf area index but did not alter leaf optical characteristics because the influence of individual leaf traits (e.g., leaf mass per area) on these properties remains highly uncertain especially under future conditions (Ollinger, 2011).

Several environmental drivers of leaf mass per area acclimation – CO_2, temperature, and nutrient limitation – will likely be modified by climate change. We estimate that the influence of temperature acclimation of leaf mass per area globally is secondary to CO_2 (Text S2.1 and Figure S1). The effect of temperature warming on leaf mass per area occurs under cold conditions; thus, the acclimation is limited to high latitude boreal regions (Figure S5). Nutrient limitation is expected to increase with CO_2 fertilization of plant growth (Norby et al., 2010; Wieder et al., 2015) and has been found to enhance leaf mass per area in manipulation experiments (Poorter et al., 2009), which could further amplify the impacts of leaf acclimation to elevated CO_2. The magnitude of leaf mass per area acclimation in response to climate change may ultimately depend upon the combined influence, including potential interaction effects, of multiple climate drivers.

Accounting for leaf acclimation in climate projections will require the ability to represent the functional relationship between leaf mass per area and its climate drivers, especially CO_2, by biome at the global scale. This remains challenging (Medlyn et al., 2015). Poorter et al.'s (2009) empirical relationship, used herein, shows that on average leaf mass per area increases with CO_2 in C_3 species. However, the proportion of variance in the magnitude of acclimation explained by this relationship is relatively low (Poorter et al., 2009), suggesting that other key drivers, such as plant type, still need to be incorporated. A mechanistic model of leaf mass per area acclimation also remains elusive. The leading hypothesis for why elevated CO_2 increases leaf mass per area is that the abundance of carbon causes nonstructural carbohydrates to accumulate in leaves (Poorter et al., 2009, 1997; Pritchard et al., 1999; Roumet et al., 1999). One possible advantage for plants of increasing leaf mass per area under elevated CO_2 is that it maintains a high level of leaf nitrogen per leaf area (gN/m^2 leaf area), an essential component of photosynthetic machinery, by counteracting a decrease in leaf nitrogen concentration (gN/g leaf) driven by larger pools of nonstructural carbohydrates (N per area = N per mass x leaf mass per area; Ishizaki et al., 2003; Luo et al., 1994; Peterson et al., 1999; Poorter et al., 1997; Stitt & Krapp, 1999). However, this process operates differently across environments, plant species, and even genotypes (Körner et al., 1997; Luo et al., 1994; Peterson et al., 1999; Poorter et al., 1997, 2009; Pritchard et al., 1999; Roumet et al., 1999; Stitt & Krapp, 1999). Further research into the underlying mechanism, influences of multiple environmental drivers, and differences in acclimation between plant types is needed to develop a representation of leaf mass per area acclimation suitable for use in Earth system models.

The climate implications of increased leaf mass per area reveal an urgent need for observational constraints on the magnitude and mechanism of leaf trait acclimation to future

climate conditions. Other structural trait acclimations that influence leaf area may have similar climate implications that require testing. Our findings suggest that the uncertainty in vegetation-climate feedbacks, and therefore climate change projections, is even larger than previously thought.

Acknowledgements

We thank M. Laguë and E. Garcia for help with model setup. We acknowledge support from the National Science Foundation AGS-1321745 and AGS-1553715 to the University of Washington. High-performance computing support from Yellowstone (ark:/85065/d7wd3xhc) was provided by NCAR's Computational and Information Systems Laboratory, sponsored by the National Science Foundation. M. K. thanks the UW Program on Climate Change Graduate Fellowship for support. Model results are available through the University of Washington Libraries ResearchWorks digital repository. The URL for the data in the ResearchWorks system is https://digital.lib.washington.edu/researchworks/handle/1773/41856.

References

Ainsworth, E. A., & Long, S. P. (2005). What have we learned from 15 years of free-air CO_2 enrichment (FACE)? A meta-analytic review of the responses of photosynthesis, canopy properties and plant production to rising CO_2. *New Phytologist*, *165*(2), 351–371. https://doi.org/10.1111/j.1469-8137.2004.01224.x

Ainsworth, E. A., & Rogers, A. (2007). The response of photosynthesis and stomatal conductance to rising [CO_2]: mechanisms and environmental interactions. *Plant, Cell and Environment*, *30*, 258–270. https://doi.org/10.1111/j.1365-3040.2007.01641.x

Anderegg, L. D., Berner, L. T., Badgley, G., Sethi, M. L., Law, B. E., & HilleRisLambers, J. (2018). Within-species patterns challenge our understanding of the leaf economics spectrum. *Ecology Letters*, *21*(5), 734–744. https://doi.org/10.1111/ele.12945

Archer, D., Eby, M., Brovkin, V., Ridgwell, A., Cao, L., Mikolajewicz, U., et al. (2009). Atmospheric lifetime of fossil fuel carbon dioxide. *Annual Review of Earth and Planetary Sciences*, *37*(1), 117–134. https://doi.org/10.1146/annurev.earth.031208.100206

Arora, V. K., Boer, G. J., Friedlingstein, P., & Eby, M. (2013). Carbon–concentration and carbon–climate feedbacks in CMIP5 Earth system models. *Journal of Climate*, *26*(15), 5289–5314. https://doi.org/10.1175/JCLI-D-12-00494.1

Betts, R. A., Boucher, O., Collins, M., Cox, P. M., Falloon, P. D., Gedney, N., et al. (2007). Projected increase in continental runoff due to plant responses to increasing carbon dioxide. *Nature*, *448*(7157), 1037–1041. https://doi.org/10.1038/nature06045

Betts, R. A., Cox, P. M., Lee, S. E., & Woodward, F. I. (1997). Contrasting physiological and structural vegetation feedbacks in climate change simulations. *Nature*, *387*(6635), 796–799. https://doi.org/10.1038/42924

Bonan, G. B. (2008). Forests and climate change: Forcings, feedbacks, and the climate benefits of forests. *Science*, *320*, 1444–1449. https://doi.org/10.1126/science.1155121

Boucher, O., Jones, A., & Betts, R. A. (2009). Climate response to the physiological impact of carbon dioxide on plants in the Met Office Unified Model HadCM3. *Climate Dynamics*, *32*(2-3), 237–249. https://doi.org/10.1007/s00382-008-0459-6

Bounoua, L., Hall, F. G., Sellers, P. J., Kumar, A., Collatz, G. J., Tucker, C. J., & Imhoff, M. L. (2010). Quantifying the negative feedback of vegetation to greenhouse warming: A modeling approach. *Geophysical Research Letters*, *37*(23). https://doi.org/10.1029/2010GL045338

Broecker, W. S., Takahashi, T., Simpson, H. J., & Peng, T. H. (1979). Fate of fossil fuel carbon dioxide and the global carbon budget. *Science*, *206*(4417), 409–418. https://doi.org/10.1126/science.206.4417.409

Butler, E. E., Datta, A., Flores-Moreno, H., Chen, M., Wythers, K. R., Fazayeli, F., et al. (2017). Mapping local and global variability in plant trait distributions. *Proceedings of the National Academy of Sciences of the United States of America*, *114*(51), E10937–E10946. https://doi.org/10.1073/pnas.1708984114

Cao, L., Bala, G., Caldeira, K., Nemani, R., & Ban-Weiss, G. (2010). Importance of carbon dioxide physiological forcing to future climate change. *Proceedings of the National Academy of Sciences of the United States of America*, *107*(21), 9513–9518. https://doi.org/10.1073/pnas.0913000107

Ciais, P., Sabine, C., Bala, G., Bopp, L., Brovkin, V., Canadell, J., et al. (2013). Carbon and other biogeochemical cycles. In *Climate change 2013: The physical science basis. Contribution of Working Group I to the Fifth Assessment Report of the Intergovernmental Panel on Climate Change* (pp. 465–570). Cambridge, UK: Cambridge University Press.

Cox, P. M., Betts, R. A., Bunton, C. B., Essery, R., Rowntree, P. R., & Smith, J. (1999). The impact of new land surface physics on the GCM simulation of climate and climate sensitivity. *Climate Dynamics*, *15*(3), 183–203. https://doi.org/10.1007/s003820050276

Cubasch, U., Wuebbles, D., Chen, D., Facchini, M. C., Frame, D., Mahowald, N., & Winther, J. G. (2013). Introduction. In T. F. Stocker, D. Qin, G. K. Plattner, M. Tignor, S. K. Allen, J. Boschung, et al. (Eds.), *Climate change 2013: The physical science basis. Contribution of Working Group I to the Fifth Assessment Report of the Intergovernmental Panel on Climate Change* (pp. 121–158). Cambridge, UK: Cambridge University Press.

Davin, E. L., & de Noblet-Ducoudré, N. (2010). Climatic impact of global-scale deforestation: Radiative versus nonradiative processes. *Journal of Climate*, *23*(1), 97–112. https://doi.org/10.1175/2009JCLI3102.1

De Kauwe, M. G., Medlyn, B. E., Zaehle, S., Walker, A. P., Dietze, M. C., Hickler, T., et al. (2013). Forest water use and water use efficiency at elevated CO_2: A model-data intercomparison at two contrasting temperate forest FACE sites. *Global Change Biology*, *19*(6), 1759–1779. https://doi.org/10.1111/gcb.12164

De Kauwe, M. G., Medlyn, B. E., Zaehle, S., Walker, A. P., Dietze, M. C., Wang, Y.-P., et al. (2014). Where does the carbon go? A model-data intercomparison of vegetation carbon allocation and turnover processes at two temperate forest free-air CO_2 enrichment sites. *New Phytologist*, *203*(3), 883–899. https://doi.org/10.1111/nph.12847

Efron, B., & Gong, G. (1983). A leisurely look at the bootstrap, the jackknife, and cross-validation. *The American Statistician*, *37*(1), 36–48. https://doi.org/10.2307/2685844

Efron, B., & Tibshirani, R. J. (1994). An introduction to the bootstrap. CRC press.

Fisher, R. A., Muszala, S., Verteinstein, M., Lawrence, P., Xu, C., McDowell, N. G., et al. (2015). Taking off the training wheels: The properties of a dynamic vegetation model without climate envelopes. *Geoscientific Model Development Discussions*, *8*(4), 3293–3357. https://doi.org/10.5194/gmdd-8-3293-2015

Friedlingstein, P., Meinshausen, M., Arora, V. K., Jones, C. D., Anav, A., Liddicoat, S. K., & Knutti, R. (2014). Uncertainties in CMIP5 climate projections due to carbon cycle feedbacks. *Journal of Climate*, *27*(2), 511–526. https://doi.org/10.1175/JCLI-D-12-00579.1

Hansen, J. E., Sato, M., Lacis, A., Ruedy, R., Tegen, I., & Matthews, E. (1998). Climate forcings in the Industrial era. *Proceedings of the National Academy of Sciences of the United States of America*, *95*(22), 12753–12758. https://doi.org/10.1073/pnas.95.22.12753

Hunke, E. C., & Lipscomb, W. H. (2010). CICE: The Los Alamos Sea Ice Model Documentation and Software User's Manual Version 4.1 LA-CC-06-012, 1–76.

Ishizaki, S., Hikosaka, K., & Hirose, T. (2003). Increase in leaf mass per area benefits plant growth at elevated CO_2 concentration. *Annals of Botany*, *91*(7), 905–914. https://doi.org/10.1093/aob/mcg097

Kattge, J., & Knorr, W. (2007). Temperature acclimation in a biochemical model of photosynthesis: A reanalysis of data from 36 species. *Plant, Cell and Environment*, *30*(9), 1176–1190. https://doi.org/10.1111/j.1365-3040.2007.01690.x

Kattge, J., Diaz, S., Lavorel, S., Prentice, I. C., Leadley, P., Bonisch, G., et al. (2011). TRY – A global database of plant traits. *Global Change Biology*, *17*, 2905–2935. https://doi.org/10.1111/j.1365-2486.2011.02451.x

Körner, C., Diemer, M., Schäppi, B., Niklaus, P., & Arnone, J. (1997). The responses of alpine grassland to four seasons of CO_2 enrichment: A synthesis. *Acta Oecologica*, *18*(3), 165–175. https://doi.org/10.1016/S1146-609X(97)80002-1

Koven, C. D., Lawrence, D. M., & Riley, W. J. (2015). Permafrost carbon−climate feedback is sensitive to deep soil carbon decomposability but not deep soil nitrogen dynamics. *Proceedings of the National Academy of Sciences of the United States of America*, *112*(12), 3752–3757. https://doi.org/10.1073/pnas.1415123112

Le Quéré, C., Andrew, R. M., Canadell, J. G., Sitch, S., Korsbakken, J. I., Peters, G. P., et al. (2016). Global carbon budget 2016. *Earth System Science Data*, *8*(2), 605–649. https://doi.org/10.5194/essd-8-605-2016

Leakey, A. D. B., Ainsworth, E. A., Bernacchi, C. J., Zhu, X., Long, S. P., & Ort, D. R. (2012). Photosynthesis in a CO_2-rich atmosphere. In *Photosynthesis in silico* (Vol. 34, pp. 733–768). Dordrecht: Springer Netherlands. https://doi.org/10.1007/978-94-007-1579-0_29

Lombardozzi, D. L., Bonan, G. B., Smith, N. G., Dukes, J. S., & Fisher, R. A. (2015). Temperature acclimation of photosynthesis and respiration: A key uncertainty in the carbon cycle-climate feedback. *Geophysical Research Letters*, *42*(20), 8624–8631. https://doi.org/10.1002/2015GL065934

Lovenduski, N. S., & Bonan, G. B. (2017). Reducing uncertainty in projections of terrestrial carbon uptake. *Environmental Research Letters*, *12*(4), 044020. https://doi.org/10.1088/1748-9326/aa66b8

Luo, Y., Field, C. B., & Mooney, H. A. (1994). Predicting responses of photosynthesis and root fraction to elevated [CO_2]a: Interactions among carbon, nitrogen, and growth. *Plant, Cell and Environment*, *17*(11), 1195–1204. https://doi.org/10.1111/j.1365-3040.1994.tb02017.x

Lusk, C. H., Reich, P. B., Montgomery, R. A., Ackerly, D. D., & Cavender-Bares, J. (2008). Why are evergreen leaves so contrary about shade? *Trends in Ecology & Evolution*, *23*(6), 299–303. https://doi.org/10.1016/j.tree.2008.02.006

Mahowald, N., Lo, F., Zheng, Y., Harrison, L., Funk, C., Lombardozzi, D., & Goodale, C. (2016). Projections of leaf area index in Earth system models. *Earth System Dynamics*, *7*(1), 211–229. https://doi.org/10.5194/esd-7-211-2016

Medlyn, B. E., Badeck, F. W., De Pury, D., Barton, C., Broadmeadow, M., Ceulemans, R., et al. (1999). Effects of elevated [CO_2] on photosynthesis in European forest species: A meta-analysis of model parameters. *Plant, Cell and Environment*, *22*(12), 1475–1495. https://doi.org/10.1046/j.1365-3040.1999.00523.x

Medlyn, B. E., Zaehle, S., De Kauwe, M. G., Walker, A. P., Dietze, M. C., Hanson, P. J., et al. (2015). Using ecosystem experiments to improve vegetation models. *Nature Climate*

Change, *5*(6), 528–534. https://doi.org/10.1038/nclimate2621

Myhre, G., Highwood, E. J., Shine, K. P., & Stordal, F. (1998). New estimates of radiative forcing due to well mixed greenhouse gases. *Geophysical Research Letters*, *25*(14), 2715–2718. https://doi.org/10.1029/98GL01908

Neale, R. B., Chen, C.-C., Gettelman, A., Lauritzen, P. H., Park, S., Williamson, D. L., Coauthors. (2012). Description of the NCAR Community Atmosphere Model (CAM 5.0). NCAR Technical Note. NCAR/TN-486+STR, 1–289.

Niinemets, Ü. (2001). Global-scale climatic controls of leaf dry mass per area, density, and thickness in trees and shrubs. *Ecology*, *82*(2), 453–469. https://doi.org/10.1890/0012-9658(2001)082[0453:GSCCOL]2.0.CO;2

Norby, R. J., Cotrufo, M. F., Ineson, P., O'Neill, E. G., & Canadell, J. G. (2001). Elevated CO_2, litter chemistry, and decomposition: A synthesis. *Oecologia*, *127*(2), 153–165. https://doi.org/10.1007/s004420000615

Norby, R. J., Sholtis, J. D., Gunderson, C. A., & Jawdy, S. S. (2003). Leaf dynamics of a deciduous forest canopy: No response to elevated CO_2. *Oecologia*, *136*(4), 574–584. https://doi.org/10.1007/s00442-003-1296-2

Norby, R. J., Warren, J. M., Iversen, C. M., Medlyn, B. E., & McMurtrie, R. E. (2010). CO_2 enhancement of forest productivity constrained by limited nitrogen availability. *Proceedings of the National Academy of Sciences of the United States of America*, *107*(45), 19368–19373. https://doi.org/10.1073/pnas.1006463107

Oleson, K. W., Lawrence, D. M., Bonan, G. B., Drewniak, B., Huang, M., Koven, C. D., et al. (2013). Technical description of the version 4.5 of the Community Land Model (CLM). NCAR Technical Note. NCAR/TN-503+STR. Retrieved from http://www.cesm.ucar.edu/models/cesm1.2/clm/CLM45_Tech_Note.pdf

Ollinger, S. V. (2011). Sources of variability in canopy reflectance and the convergent properties of plants. *New Phytologist*, *189*(2), 375–394. https://doi.org/10.1111/j.1469-8137.2010.03536.x

Patton, A. (2007). Automatic block length selection procedure. Retrieved June 28, 2016, from http://public.econ.duke.edu/~ap172/opt_block_length_REV_dec07.txt

Patton, A., Politis, D. N., & White, H. (2009). Correction to "Automatic block-length selection for the dependent bootstrap" by D. Politis and H. White. *Econometric Reviews*. https://doi.org/10.1080/07474930802459016

Pavlick, R., Drewry, D. T., Bohn, K., Reu, B., & Kleidon, A. (2013). The Jena Diversity-Dynamic Global Vegetation Model (JeDi-DGVM): A diverse approach to representing terrestrial biogeography and biogeochemistry based on plant functional trade-offs.

Biogeosciences, *10*(6), 4137–4177. https://doi.org/10.5194/bg-10-4137-2013

Peterson, A. G., Ball, J. T., Luo, Y., Field, C. B., Curtis, P. S., Griffin, K. L., et al. (1999). Quantifying the response of photosynthesis to changes in leaf nitrogen content and leaf mass per area in plants grown under atmospheric CO_2 enrichment. *Plant, Cell and Environment*, *22*(9), 1109–1119. https://doi.org/10.1046/j.1365-3040.1999.00489.x

Politis, D. N., & Romano, J. P. (1994). The stationary bootstrap. *Journal of the American Statistical Association*, *89*(428), 1303–1313. https://doi.org/10.2307/2290993

Politis, D. N., & White, H. (2004). Automatic block-length selection for the dependent bootstrap. *Econometric Reviews*, *23*(1), 53–70. https://doi.org/10.1081/ETC-120028836

Pongratz, J., Reick, C. H., Raddatz, T., & Claussen, M. (2010). Biogeophysical versus biogeochemical climate response to historical anthropogenic land cover change. *Geophysical Research Letters*, *37*, L08702. https://doi.org/10.1029/2010GL043010

Poorter, H., Berkel, Y. V., Baxter, R., Hertog, J. D., Dijkstra, P., Gifford, R. M., et al. (1997). The effect of elevated CO_2 on the chemical composition and construction costs of leaves of 27 C_3 species. *Plant, Cell and Environment*, *20*(4), 472–482. https://doi.org/10.1046/j.1365-3040.1997.d01-84.x

Poorter, H., Niinemets, Ü., Poorter, L., Wright, I. J., & Villar, R. (2009). Causes and consequences of variation in leaf mass per area (LMA): A meta-analysis. *New Phytologist*, *182*, 565–588. https://doi.org/10.1111/j.1469-8137.2009.02830.x

Pritchard, S. H., Rogers, H. O., Prior, S. A., & Peterson, C. M. (1999). Elevated CO_2 and plant structure: A review. *Global Change Biology*, *5*(7), 807–837. https://doi.org/10.1046/j.1365-2486.1999.00268.x

Pu, B., & Dickinson, R. E. (2012). Examining vegetation feedbacks on global warming in the Community Earth System Model. *Journal of Geophysical Research*, *117*, D20110. https://doi.org/10.1029/2012JD017623

Quilis, E. M. (2015). Bootstrapping time series. Version 1.0. Retrieved June 17, 2016, from https://www.mathworks.com/matlabcentral/fileexchange/53701-bootstrapping-time-series

Reich, P. B., Rich, R. L., Lu, X., Wang, Y.-P., & Oleksyn, J. (2014). Biogeographic variation in evergreen conifer needle longevity and impacts on boreal forest carbon cycle projections. *Proceedings of the National Academy of Sciences of the United States of America*, *111*(38), 13703–13708. https://doi.org/10.1073/pnas.1216054110

Reichstein, M., Bahn, M., Mahecha, M. D., Kattge, J., & Baldocchi, D. D. (2014). Linking plant and ecosystem functional biogeography. *Proceedings of the National Academy of Sciences of the United States of America*, *111*(38), 13697–13702. https://doi.org/10.1073/pnas.1216065111

Rogers, A., Medlyn, B. E., Dukes, J. S., Bonan, G., Caemmerer, von, S., Dietze, M. C., et al. (2017). A roadmap for improving the representation of photosynthesis in Earth system models. *The New Phytologist*, *213*(1), 22–42. https://doi.org/10.1111/nph.14283

Roumet, C., Laurent, G., & Roy, J. (1999). Leaf structure and chemical composition as affected by elevated CO_2: Genotypic responses of two perennial grasses. *New Phytologist*, *143*(1), 73–81. https://doi.org/10.1046/j.1469-8137.1999.00437.x

Said, S. E., & Dickey, D. A. (1984). Testing for unit roots in autoregressive-moving average models of unknown order. *Biometrika*, *71*(3), 599–607. https://doi.org/10.1093/biomet/71.3.599

Scheiter, S., Langan, L., & Higgins, S. I. (2013). Next-generation dynamic global vegetation models: Learning from community ecology. *New Phytologist*, *198*(3), 957–969. https://doi.org/10.1111/nph.12210

Sellers, P. J., Bounoua, L., Collatz, G. J., Randall, D. A., Dazlich, D. A., Los, S. O., et al. (1996). Comparison of radiative and physiological effects of doubled atmospheric CO_2 on climate. *Science*, *271*(5254), 1402–1406. https://doi.org/10.1126/science.271.5254.1402

Smith, N. G., & Dukes, J. S. (2013). Plant respiration and photosynthesis in global-scale models: incorporating acclimation to temperature and CO_2. *Global Change Biology*, *19*(1), 45–63. https://doi.org/10.1111/j.1365-2486.2012.02797.x

Smith, N. G., Lombardozzi, D., Tawfik, A., Bonan, G., & Dukes, J. S. (2017). Biophysical consequences of photosynthetic temperature acclimation for climate. *Journal of Advances in Modeling Earth Systems*. https://doi.org/10.1002/2016MS000732

Stitt, M., & Krapp, A. (1999). The interaction between elevated carbon dioxide and nitrogen nutrition: The physiological and molecular background. *Plant, Cell and Environment*, *22*(6), 583–621. https://doi.org/10.1046/j.1365-3040.1999.00386.x

Strain, B. R., & Bazzaz, F. A. (1983). Terrestrial plant communities. In E. R. Lemon (Ed.), *CO_2 and plants* (pp. 177–222). Boulder, Colorado: Westview;(United States).

Swann, A. L. S., Hoffman, F. M., Koven, C. D., & Randerson, J. T. (2016). Plant responses to increasing CO_2 reduce estimates of climate impacts on drought severity. *Proceedings of the National Academy of Sciences of the United States of America*, *113*(36), 10019–10024. https://doi.org/10.1073/pnas.1604581113

Taylor, G., Tallis, M. J., Giardina, C. P., Percy, K. E., Miglietta, F., Gupta, P. S., et al. (2008). Future atmospheric CO_2 leads to delayed autumnal senescence. *Global Change Biology*, *14*(2), 264–275. https://doi.org/10.1111/j.1365-2486.2007.01473.x

Van Bodegom, P. M., Douma, J. C., Witte, J. P. M., Ordoñez, J. C., Bartholomeus, R. P., &

Aerts, R. (2012). Going beyond limitations of plant functional types when predicting global ecosystem-atmosphere fluxes: Exploring the merits of traits-based approaches. *Global Ecology and Biogeography*, *21*(6), 625–636. https://doi.org/10.1111/j.1466-8238.2011.00717.x

Verheijen, L. M., Aerts, R., Brovkin, V., Cavender-Bares, J., Cornelissen, J. H. C., Kattge, J., & van Bodegom, P. M. (2015). Inclusion of ecologically based trait variation in plant functional types reduces the projected land carbon sink in an Earth system model. *Global Change Biology*, *21*(8), 3074–3086. https://doi.org/10.1111/gcb.12871

Verheijen, L. M., Brovkin, V., Aerts, R., Bonisch, G., Cornelissen, J. H. C., Kattge, J., et al. (2013). Impacts of trait variation through observed trait–climate relationships on performance of an Earth system model: A conceptual analysis. *Biogeosciences*, *10*(8), 5497–5515. https://doi.org/10.5194/bg-10-5497-2013

Way, D. A., Oren, R., & Kroner, Y. (2015). The space-time continuum: The effects of elevated CO_2 and temperature on trees and the importance of scaling. *Plant, Cell and Environment*, *38*(6), 991–1007. https://doi.org/10.1111/pce.12527

Wei, Z., Yoshimura, K., Wang, L., Miralles, D. G., Jasechko, S., & Lee, X. (2017). Revisiting the contribution of transpiration to global terrestrial evapotranspiration. *Geophysical Research Letters*, *44*(6), 2792–2801. https://doi.org/10.1002/2016GL072235

White, M. A., Thornton, P. E., Running, S. W., & Nemani, R. R. (2000). Parameterization and sensitivity analysis of the BIOME-BGC terrestrial ecosystem model: Net primary production controls. *Earth Interactions*, *4*(3), 1–85. https://doi.org/10.1175/1087-3562(2000)004<0003:PASAOT>2.0.CO;2

Wieder, W. R., Cleveland, C. C., Smith, W. K., & Todd-Brown, K. (2015). Future productivity and carbon storage limited by terrestrial nutrient availability. *Nature*, *8*(6), 441–444. https://doi.org/10.1038/ngeo2413

Wright, I. J., Reich, P. B., Westoby, M., Ackerly, D. D., Baruch, Z., Bongers, F., et al. (2004). The worldwide leaf economics spectrum. *Nature*, *428*(6985), 821–827. https://doi.org/10.1038/nature02403

Zhou, B., & Wong, W. H. (2011). A bootstrap-based non-parametric ANOVA method with applications to factorial microarray data. *Statistica Sinica*, *21*(2), 495–514. https://doi.org/10.5705/ss.2011.023a

Tables

Table 1. Annual Mean Change Over Land due to Leaf Trait Acclimation (CCLMA-CC)

	Global		S. extratropics		Tropics		N. extratropics	
Biogeophysical warming (°C)	0.3	(0.1%)	0.3	(0.1%)	0.3	(0.1%)	0.4	(0.1%)
Net primary productivity (PgC/year)	-5.8	(-6.4%)	-0.8	(-9.1%)	-2.5	(-6.1%)	-2.1	(-6.2%)
Leaf area index (m^2/m^2)	-0.9	(-26.0%)	-0.8	(-24.0%)	-1.0	(-24.3%)	-1.0	(-27.4%)
Evapotranspiration (W/m^2)	-0.7	(-1.5%)	-0.9	(-1.6%)	-1.2	(-1.6%)	-0.4	(-1.1%)
Transpiration (W/m^2)	-1.4	(-5.8%)	-1.9	(-7.2%)	-1.7	(-4.6%)	-1.1	(-6.7%)
Leaf Evaporation (W/m^2)	-0.8	(-8.6%)	-0.7	(-8.5%)	-1.3	(-8.3%)	-0.5	(-9.0%)
Soil Evaporation (W/m^2)	1.4	(9.5%)	1.6	(7.0%)	1.9	(10.6%)	1.3	(9.9%)
Absorbed solar radiation (W/m^2)	0.6	(0.4%)	0.8	(0.5%)	0.6	(0.4%)	0.6	(0.4%)

Note. All changes significant at the 95% level. Percent change ((CCLMA-CC)/CC) in parentheses. Confidence intervals reported in Table S2.

Figures

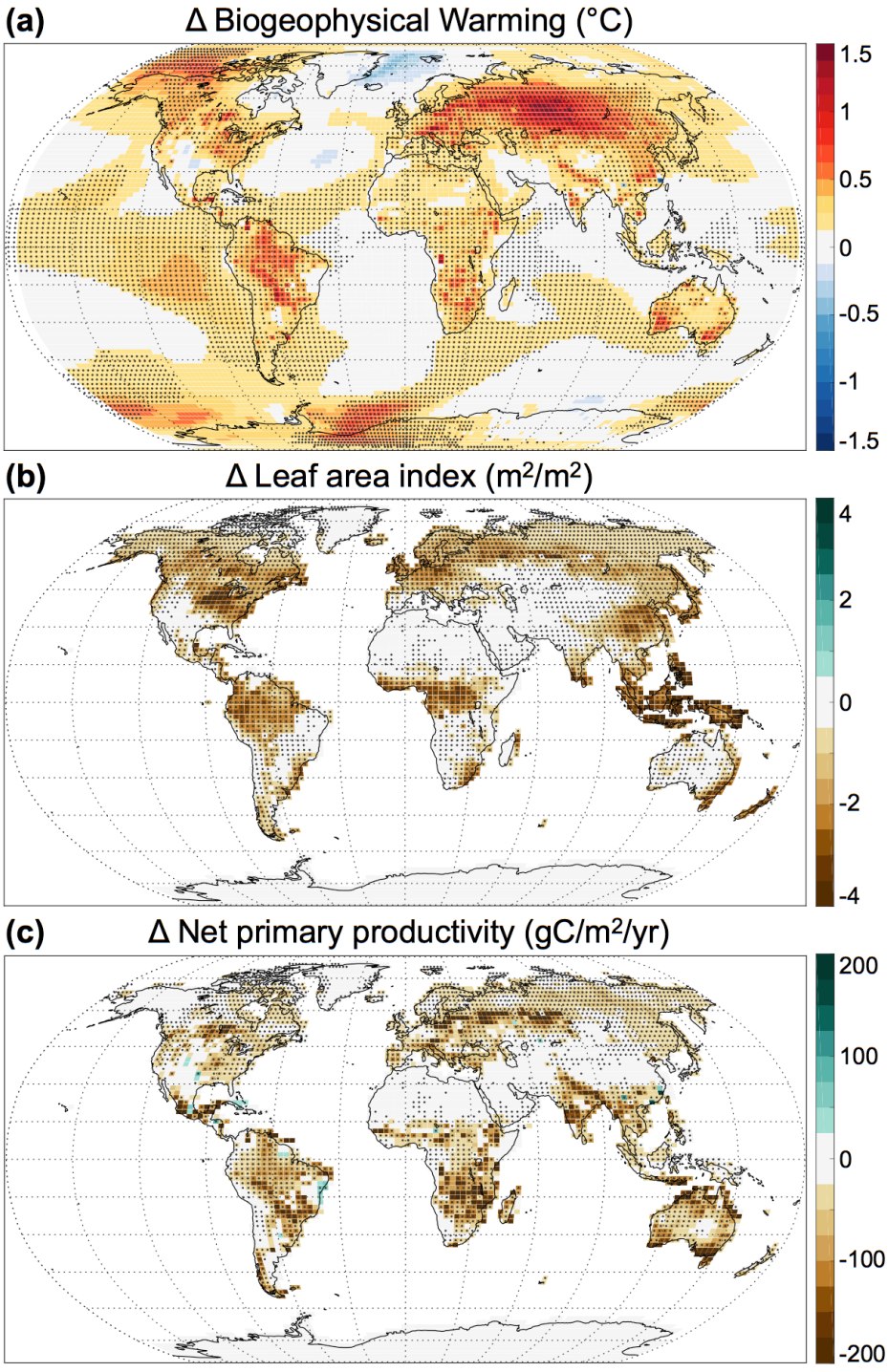

Figure 1 Annual mean change due to leaf acclimation to CO_2 (CCLMA-CC) of (a) biogeophysical warming (°C); (b) leaf area index (m^2/m^2); and (c) net primary productivity (gC/m^2/year). Stippling indicates significance at the 95% level.

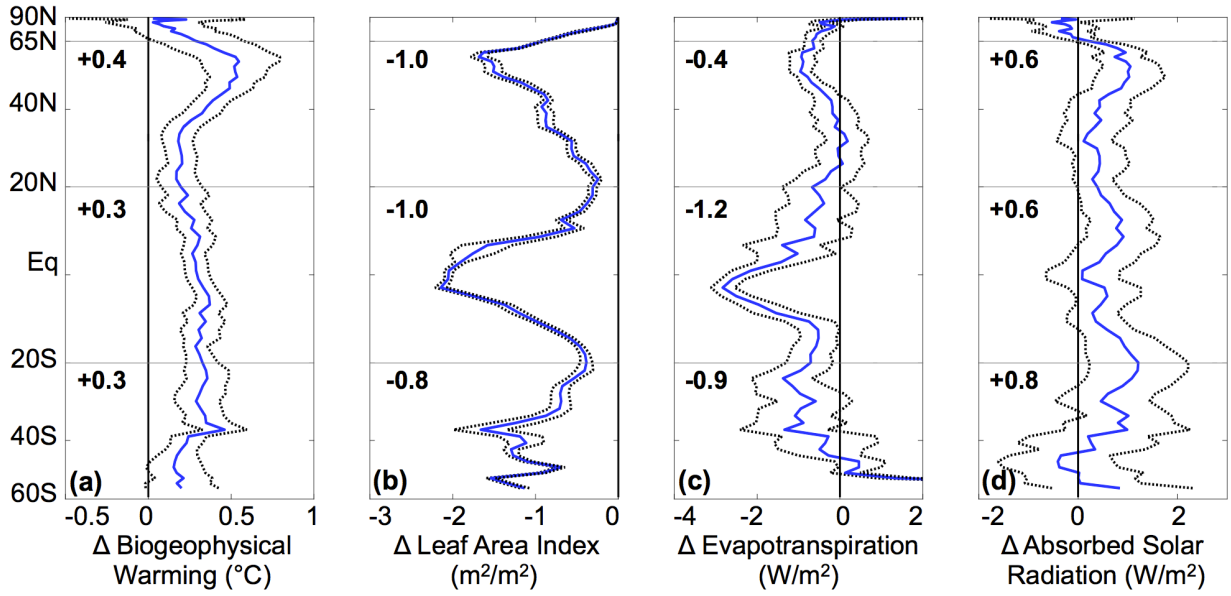

Figure 2 Zonal annual mean change over land due to leaf acclimation to CO_2 (CCLMA-CC) of (a) biogeophysical warming (°C); (b) leaf area index (m^2/m^2); (c) evapotranspiration (W/m^2); and (d) net solar radiation absorbed at the surface (W/m^2). The mean difference is shown in blue, along with the 95% bootstrap confidence interval (black dashed) and average zonal mean change on land (bold numbers) for each latitude band (bounded by gray lines).

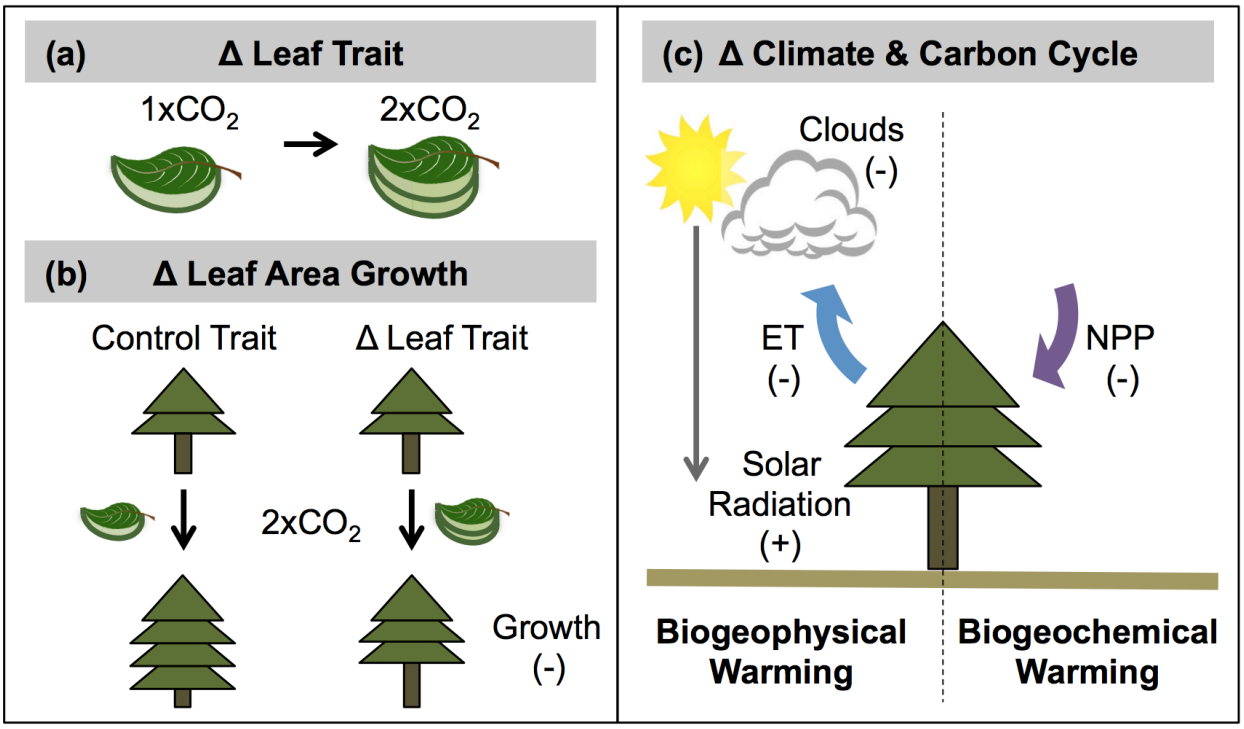

Figure 3 Schematic summary of changes due to leaf trait acclimation to elevated CO_2. (a) Leaf mass per area increases in response to elevated CO_2 in C_3 plants (CCLMA). Light green represents leaf mass (gC); dark green represents leaf area (m^2). (b) Leaf trait acclimation reduces leaf area growth in response to elevated CO_2 compared to the climate change control (CCLMA-CC). (c) Lower leaf area growth drives additional biogeophysical warming over land compared to the climate change control (CCLMA-CC) by diminishing evapotranspirative (ET) cooling, reducing cloud cover, and enhancing solar radiation absorbed by the surface. It also decreases net primary productivity (NPP), which can drive additional anomalous biogeochemical warming by reducing land uptake of CO_2 from the atmosphere. A positive sign (+) indicates an increase and a negative sign (-) represents a decrease in response to leaf trait acclimation (CCLMA-CC).

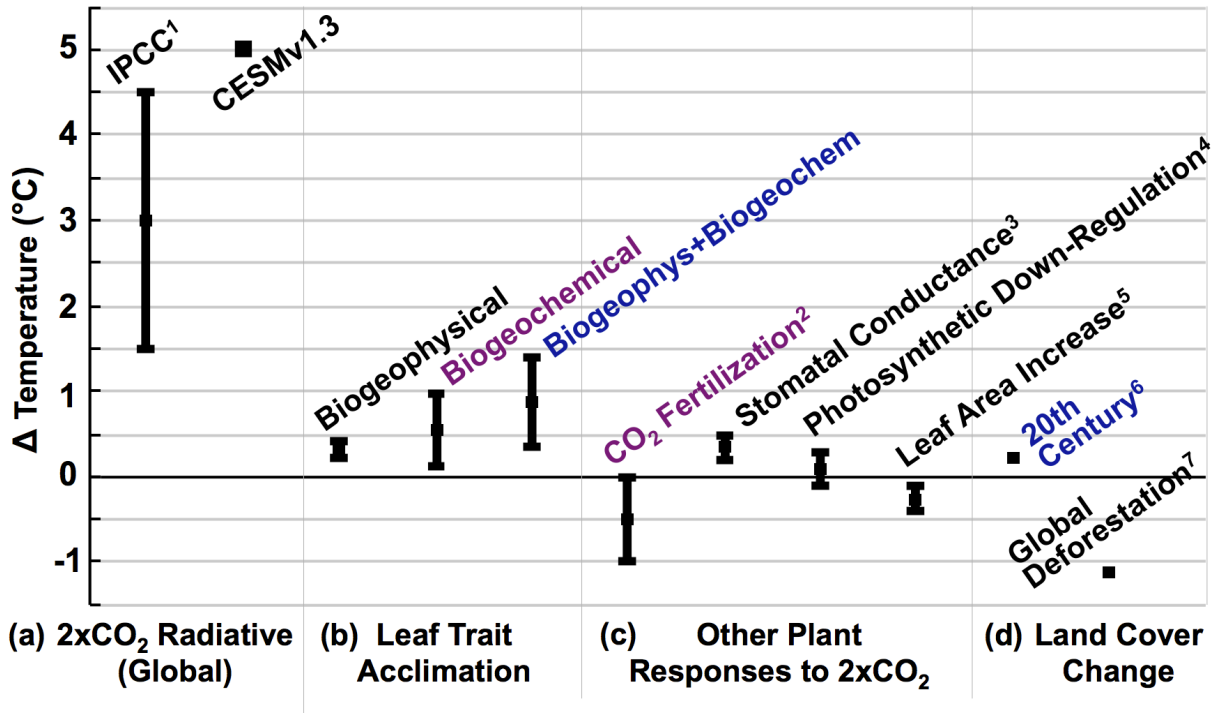

Figure 4 Comparison of temperature changes in response to a doubling of CO_2 (a) radiative forcing; (b) acclimation of leaf mass per area; (c) other plant responses; and (d) land cover change with color of text indicating biogeophysical warming (black text), biogeochemical warming (purple text), and combined warming (blue text). Estimates were drawn from the literature as follows: [1]Ciais et al. (2013) range based on observations of 20th century climate change, paleoclimate, Coupled Model Intercomparison Project Phase 5 climate models, and feedback analysis; [2]Estimated temperature response to radiative forcing from carbon-concentration feedback parameters for land across Coupled Model Intercomparison Project Phase 5 models (Arora et al., 2013) and CO_2 doubling in this study (355 to 710 ppm); [3]Mean responses across studies (Cao et al., 2010; Pu & Dickinson, 2012; Sellers et al., 1996); [4]Mean responses across studies (Bounoua et al., 2010; Pu & Dickinson, 2012); [5]Mean responses across studies (Bounoua et al., 2010; Pu & Dickinson, 2012); [6]Pongratz et al. (2010); and [7]Davin and de Noblet-Ducoudré (2010). IPCC = Intergovernmental Panel on Climate Change.

Supporting Information for

Leaf Trait Acclimation Amplifies Simulated Climate Warming in Response to Elevated Carbon Dioxide

Marlies Kovenock[1] and Abigail L. S. Swann[2,1]

[1]Department of Biology, University of Washington, Seattle, WA, USA

[2]Department of Atmospheric Sciences, University of Washington, Seattle, WA, USA

Contents of this file

Text S1. Materials and Methods

1.1 Nitrogen Cycle

As the default model's interactive nitrogen cycle breaks the relationship between transpiration fluxes and gross primary productivity (De Kauwe et al., 2013) we disabled it and represented nitrogen limitation with a fractional reduction in the rate of photosynthesis for each plant functional type following the methods of Koven et al. (2015).

1.2 CO_2 Acclimation of Leaf Mass per Area Estimation and Implementation

We estimated the plausible extent of leaf mass per area acclimation using Poorter et al.'s (2009) meta-analysis of approximately 200 studies of leaf mass per area response to CO_2 level. Specifically, we added the approximate interquartile range for the response of leaf mass per area to a doubling of CO_2 in all plants (no interquartile range for C_3 plants was reported) to the median response for C_3 plants. The resulting level of change, a one-third increase in leaf mass per area, was implemented by directly modifying the model parameter controlling leaf mass per area at the top of the canopy. This model parameter, SLA_O, represents specific leaf area (m^2 leaf area/g leaf carbon), the inverse of leaf mass per area. We therefore multiplied the SLA_O parameter for all C_3 plant types by 0.75 to implement a one-third increase in leaf mass per area.

As formulated by default, increasing leaf mass per area in this Earth system model raises area-based maximum photosynthetic rates ($\mu mol/m^2/s$) as follows:

$$V_{cmax25} = \alpha \, LMA / CN_L \qquad \text{(Eqn 1)}$$

where V_{cmax25} is the maximum rate of carboxylation at 25° C ($\mu mol\ C/m^2/s$), LMA is the leaf mass per area (gC/m^2 leaf area), CN_L is the leaf carbon-to-nitrogen ratio (gC/gN), and α accounts for the amount of nitrogen in Rubisco and the specific activity of Rubisco. Other area-based maximum photosynthetic rate parameters (J_{max25}, T_{p25}) are calculated in proportion to V_{cmax25}. In all but one simulation (CCLMAPS), we maintained control levels of area-based maximum photosynthetic rates by increasing the parameter values for CN_L (leaf gC/gN) for each C_3 plant type by one third. This change encompasses both increases in CN_L and decreases in the fraction of nitrogen in Rubisco, which have been observed in response to elevated CO_2 in manipulation experiments (reviewed in Ainsworth & Long, 2005; Leakey et al., 2012; Way et al., 2015). Prior studies have identified trait-climate relationships in the literature that suggest that V_{cmax25} and J_{max25} decrease with CO_2 (Ainsworth & Rogers, 2007; Medlyn et al., 1999). However, estimating an exact magnitude of acclimation remains challenging because empirical relationships conflate the physiological effects of CO_2, nitrogen limitation, and altered within-plant nitrogen allocation (Rogers et al., 2017; Smith & Dukes, 2013). We chose here to make a conservative estimate that maximum photosynthetic rates stay constant as

CO_2 increases. This approach is conservative as most estimates predict a decrease in maximum photosynthetic rates which would enhance the climate impacts of leaf mass per area acclimation by further reducing the increase in leaf area in response to elevated CO_2. The CCLMAPS simulation tested the sensitivity of climate impacts to a simultaneous one-third increase in maximum photosynthetic rates.

1.3 Temperature Acclimation of Leaf Mass per Area Estimation and Implementation

We estimated the potential extent of leaf mass per area acclimation to temperature using biome-specific acclimation relationships from Poorter et al.'s (2009) meta-analysis of 40 studies and the growing season temperature change due to doubling CO_2 (CC - CTRL; northern hemisphere JJA and southern hemisphere DJF) at each gridcell. We estimated the upper bound of leaf mass per area response to temperature by adding the interquartile range for all plant types reported by Poorter et al. (2009) to the biome-specific median response (biome-specific interquartile ranges were not reported). The magnitude of temperature acclimation was not sensitive to interannual variability in CC - CTRL growing season temperature.

We found that temperature could be an influential driver of leaf mass per area acclimation in boreal and arctic biomes (Fig. S5a). This is because temperature acclimation occurs when leaves warm from growth-limiting cold temperatures to temperatures suitable for growth (Poorter et al., 2009). The acclimation response declines to zero when warming begins from temperatures closer to those suitable for growth (Poorter et al., 2009). Growing season temperatures below this threshold occur primarily in boreal and arctic biomes in our simulation. Using a threshold of at least 10% response we found that four plant functional types - boreal needleleaf evergreen and deciduous trees, boreal deciduous shrubs, and C_3 arctic grasses - cover 90% of the vegetated area that we estimate could be impacted by leaf mass per area acclimation to temperature (Fig. S5b).

To test the climate influence of temperature acclimation on our results, we use an experiment (TCCLMA) that includes a conservative estimate of the upper bound of leaf mass per area acclimation to both temperature and CO_2. The TCCLMA simulation is identical to CCLMA ($2xCO_2$; +1/3 leaf mass per area in C_3 plants) except that leaf mass per area of four plant functional types - boreal needleleaf evergreen and deciduous trees, boreal deciduous shrubs, and C_3 arctic grasses - were held at control (CTRL) levels. The corresponding average response of leaf mass per area acclimation to temperature alone was -15% for gridcells with temperature acclimation. Combining the acclimation of leaf mass per area to CO_2 (+33%) with the decrease due to temperature acclimation (average value -15%) results in an average overall increase of +13%. We therefore conservatively left leaf mass per area values at control levels for these four plant types, representing an implied 25% decrease in leaf mass per area due to temperature.

This approach included a number of assumptions but offered the best estimate of leaf mass per area temperature acclimation influences on climate and carbon cycling given the options. It assumes that the temperature acclimation relationship reported by Poorter et al. (2009) holds at temperatures below 7°C, despite lack of data below this point; that as shown by Poorter et al. (2009, Fig. 5j) there is no response above 18°C; and, based on the underlying mechanisms of temperature limiting leaf expansion and sink growth (Poorter et al., 2009), that growing season rather than annual mean temperature is the driver. It also assumes that temperature and CO_2 acclimation are additive (no interaction effect).

1.4 Statistical Analysis

Several variables had time series that were non-normally distributed and temporally autocorrelated. We therefore used stationary bootstrap methods (Politis & Romano, 1994; Quilis, 2015) with n = 50,000 to test for differences. The optimal block length for each stationary bootstrap was determined by automatic estimation (Patton, 2007; Patton et al., 2009; Politis & White, 2004). Time series that failed the Augmented Dickey-Fuller test for stationarity (Said & Dickey, 1984 and Matlab version 2015b adftest function) were de-trended prior to bootstrap analysis. Differences were considered significant at the 95% level using the percentile method (Efron & Gong, 1983; Efron & Tibshirani, 1994). Confidence intervals for average annual means and differences were constructed from their bootstrap distributions. T-test and Non-parametric Analysis of Variance (Zhou & Wong, 2011 modified to use stationary bootstrap) analyses support the reported findings and conclusions.

We tested for spatial relationships between variables at the gridcell scale using simple, multiple, and stepwise linear regression methods on annual mean values (CCLMA - CC). Only continental land gridcells (no ocean or coast) that were a least 40% vegetated were included in the regression analysis. Results were not sensitive to the selected percentage vegetation. Relationships were considered significant at the 95% level.

Text S2. Results

2.1 Temperature Acclimation of Leaf Mass per Area

Observations of leaf acclimation show that warming temperatures and rising CO_2 levels have opposing influences on leaf mass per area. As such, warming temperatures could be hypothesized to offset the influence of CO_2 on leaf mass per area and the resulting climate and carbon cycling impacts. However, temperature acclimation of leaf mass per area only occurs at low temperatures (Poorter et al., 2009) and is therefore limited to boreal and arctic regions.

We quantified the influence of temperature acclimation on our CO_2 acclimation results using a simulation that represents the potential extent of leaf mass per area acclimation to both temperature and CO_2 (TCCLMA). Specifically, we compared the differences in the change from the climate change control between two leaf mass per area acclimation cases: leaf mass per area acclimation to CO_2 alone (CCLMA - CC) and leaf mass per area acclimation to both CO_2 and temperature (TCCLMA - CC).

We found that temperature acclimation of leaf mass per area did not significantly alter the additional warming beyond the climate change control induced by CO_2 acclimation of leaf mass per area. Physical warming was unaltered at the global and latitude band scales (TCCLMA - CC ≈ CCLMA - CC) because temperature acclimation of leaf mass per area did not significantly offset changes in evapotranspiration and solar radiation absorbed at the surface, despite slightly compensating for changes in leaf area index (Fig. S1). Furthermore, temperature acclimation offset only a small portion (~1 PgC/yr) of the net primary productivity change induced by CO_2 acclimation (TCCLMA - CC; -5.0 PgC/yr, $CI_{95\%}$ -4.7 to -5.3). Thus, our estimate of additional biogeochemical warming due to leaf mass per area acclimation was also similar (+0.1 to +0.9°C over 100 years for TCCLMA - CC compared to +0.1 to +1.0°C over 100 years for CCLMA - CC).

2.2 Historical Climate Sensitivity to Leaf Mass per Area Change

We found that the influence of historical leaf mass per area acclimation on climate is likely to be small. From the relationship reported by Poorter et al. (2009), we estimated that the largest potential extent of historical leaf mass per area change compared to the pre-industrial period (from 280ppm CO_2 to 355ppm) is +8%. We tested a much larger one-third increase in leaf mass per area for historical simulations at the control CO_2 concentration of 355ppm (LMA: 1xCO_2, +1/3 leaf mass per area). This experiment showed that a stronger than expected increase in leaf mass per area did not significantly alter historical temperature over land (LMA - CTRL; -0.1°C over land, $CI_{95\%}$ 0 to -0.2; -0.2°C globally, $CI_{95\%}$ -0.1 to -0.2).

The effect of leaf mass per area change in the historical period is limited for two reasons. First, the decrease in leaf area in response to a one-third increase in leaf mass per area was smaller at historical CO_2 (LMA - CTRL: -0.67 m^2/m^2, $CI_{95\%}$ -0.65 to 0.69) than at future CO_2 (CCLMA - CTRL). This smaller change in leaf area when beginning from low initial leaf area is consistent with our findings under future CO_2 conditions (see Results, Fig. S2). The small change in leaf area at historical CO_2 levels muted the decrease in evapotranspiration (LMA - CTRL: -0.6 W/m^2, $CI_{95\%}$ -0.4 to -0.8) compared to the change at future CO_2 levels (CCLMA - CC). Second, the change in solar radiation absorbed at the surface was reduced in the historical simulations (LMA - CTRL; -0.3 W/m^2, $CI_{95\%}$ -0.1 to -0.6) compared to future simulations (CCLMA - CC), as reduced leaf area increased albedo (as measured by a change in clear-sky shortwave radiation absorbed at the surface of -0.2 W/m^2, $CI_{95\%}$ -0.1 to -0.4). Overall, the small decrease in

178 solar radiation absorbed at the surface and small increase in evapotranspiration resulted in
179 a near zero change in temperature.
180 Historical net primary productivity was significantly decreased in response to the
181 one-third leaf mass per area increase (-6.9 PgC/yr, $CI_{95\%}$ -6.6 to -7.2). However, this
182 value likely overestimates the decrease in productivity by a factor of four, as the
183 predicted 8% increase in leaf mass per area for historical climate change is approximately
184 one fourth of the experimental change of 33%. We therefore suggest that -2 PgC/yr is a
185 more reasonable ballpark estimate for the sensitivity of simulated productivity to leaf
186 mass per area change at historical CO_2. We also note that while the LMA experiment
187 (355ppm CO_2, +1/3 leaf mass per area) is useful for testing the model sensitivity to
188 changes in leaf mass per area at a historical CO_2 concentration, we do not expect leaf
189 mass per area to differ from the control values at 355ppm because these values are based
190 on observations of leaf mass per area during the present day (White et al., 2000).
191
192 ***2.3 Acclimation Altered Balance between Biogeophysical and Biogeochemical***
193 ***Warming***
194 Leaf mass per area represents the conversion factor between carbon available for
195 leaf growth and leaf area. Thus increasing leaf mass per area in response to rising CO_2
196 alters the balance between biogeophysical and biogeochemical warming by altering the
197 total leaf area displayed for a given amount of productivity. Plants could overcome this
198 reduced leaf area by increasing maximum photosynthetic rates. We quantified the
199 approximate increase in maximum photosynthetic rates and productivity required to
200 offset the biogeophysical warming induced by leaf acclimation to CO_2 using a simulation
201 that simultaneously increased area-based maximum photosynthetic rates (V_{cmax25}, J_{max25},
202 T_{p25}) and leaf mass per area by one third (CCLMAPS) compared to the control climate
203 change simulation (CC).
204 The greater photosynthetic capacity increased global net primary productivity by
205 +9 PgC/yr ($CI_{95\%}$ 8 to 9) compared to the control climate change simulation (CCLMAPS
206 - CC) and +14 PgC/yr ($CI_{95\%}$ 14 to 15) compared to the leaf acclimation simulation
207 (CCLMAPS - CCLMA). This large increase in productivity mitigated approximately half
208 of the decline in global leaf area index incurred due to leaf mass per area acclimation
209 (leaf area index decreased by -14% in CCLMAPS - CC compared to -26% in CCLMA -
210 CC). While leaf area decline was not fully compensated for by increasing photosynthetic
211 rates, total evapotranspiration was no longer significantly reduced compared to the
212 control climate change simulation (CCLMAPS - CC). Transpiration remained unchanged
213 and decreased evaporation from leaf surfaces (CCLMAPS - CC; -0.4 W/m^2, $CI_{95\%}$ -0.4 to
214 -0.5) was compensated for by an increase in evaporation from the soil (+0.4 W/m^2, $CI_{95\%}$
215 +0.2 to +0.5). The albedo of the land surface increased slightly globally (-0.3 W/m^2,
216 $CI_{95\%}$ -0.1 to -0.4) compared to the climate change control consistent with the change in
217 leaf area but did not significantly alter the amount of solar radiation absorbed at the

surface (-0.2 W/m^2, $CI_{95\%}$ -0.6 to +0.1). As a result, the biogeophysical warming of the land surface due to a one-third increase in leaf mass per area (CCLMA - CC) was mitigated by a proportional increase in maximum photosynthetic rates (CCLMAPS - CC; -0.1°C, $CI_{95\%}$ 0 to -0.2;). Thus, a large increase in productivity above that estimated in our control climate change simulation offset the biogeophysical warming due to leaf acclimation. However, leaf mass per area acclimation altered the balance between productivity and biogeophysical land surface processes.

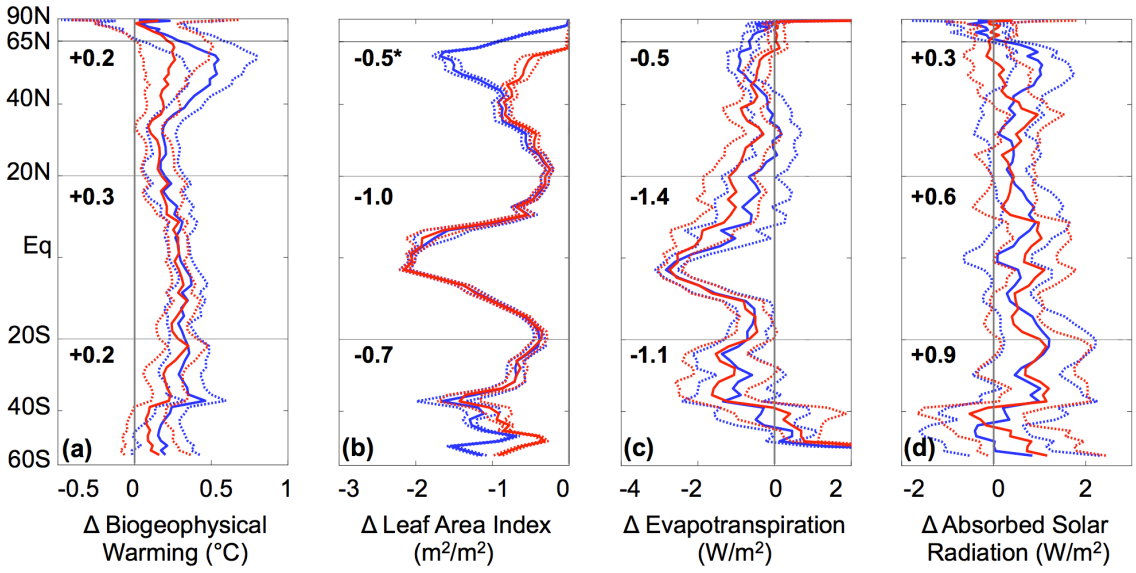

Figure S1. Zonal annual mean change over land due to leaf mass per area acclimation to temperature and CO_2 (red, TCCLMA - CC) and leaf mass per area acclimation to CO_2 alone (blue, CCLMA - CC) of (a) biogeophysical warming (°C); (b) leaf area index (m^2/m^2); (c) evapotranspiration (W/m^2); and (d) net solar radiation absorbed at the surface (W/m^2). Mean differences are shown as solid lines, along with the 95% bootstrap confidence interval (dashed lines). Average zonal mean change on land due to leaf acclimation to temperature and CO_2 (bold numbers) for each latitude band (bounded by gray lines). Latitude band differences between (CCLMA - CC) and (TCCLMA - CC) significant at the 95% level indicated with asterisk (*).

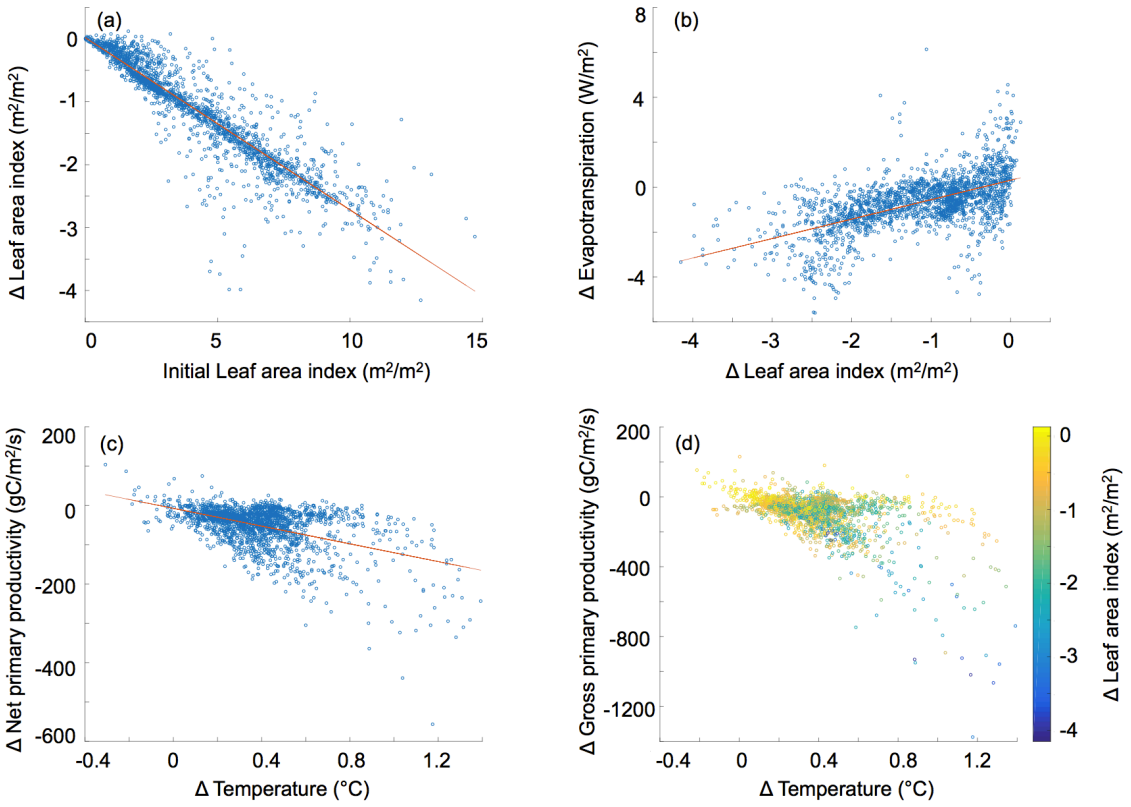

Figure S2. Scatterplot of gridcell level (a) initial leaf area index (CC) and the change in leaf area in response to leaf acclimation to CO_2 (r = -0.91, R^2 = 0.83); (b) the changes in leaf area and evapotranspiration (r = 0.57, R^2 = 0.32); (c) the changes in temperature and net primary productivity (r = -0.49, R^2 = 0.24); and (d) the changes in temperature, leaf area index, and gross primary productivity (multiple regression R^2 = 0.32). Ordinary least squares regression lines plotted in red (a-c). All changes are CCLMA - CC.

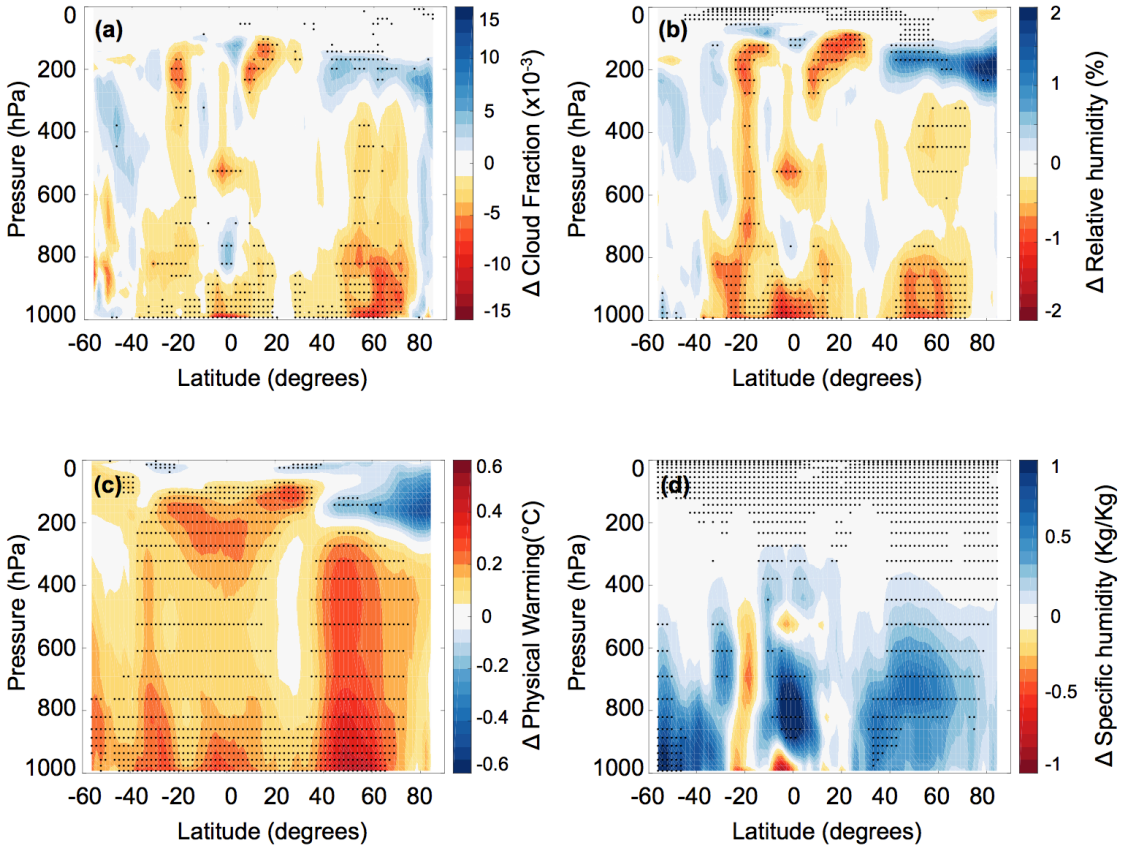

Figure S3. Zonal annual mean change over land due to leaf acclimation to CO_2 of (a) cloud fraction; (b) relative humidity (%); (c) biogeophysical warming (°C); and (d) specific humidity (Kg Water/Kg). Stippling indicates significance at the 95% level.

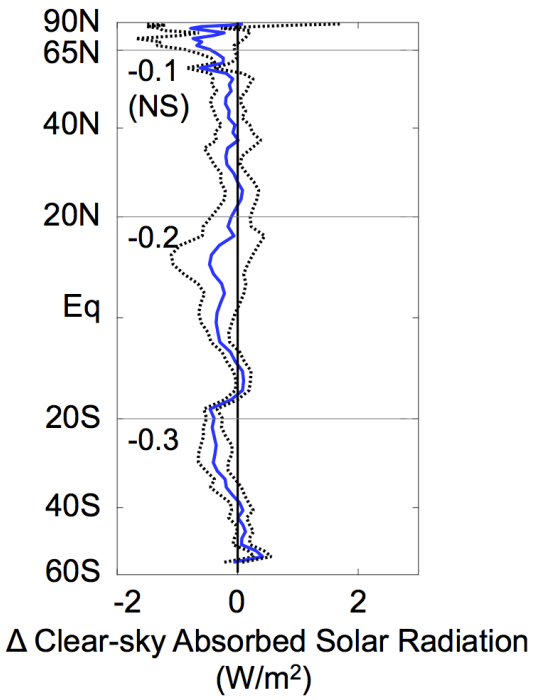

Figure S4. Zonal annual mean change over land due to leaf acclimation (CCLMA - CC) of clear-sky solar radiation absorbed at the surface (W/m^2). The mean difference is shown in blue, along with the 95% bootstrap confidence interval (dashed black) and average zonal mean change on land (bold numbers) for each latitude band (bounded by gray lines).

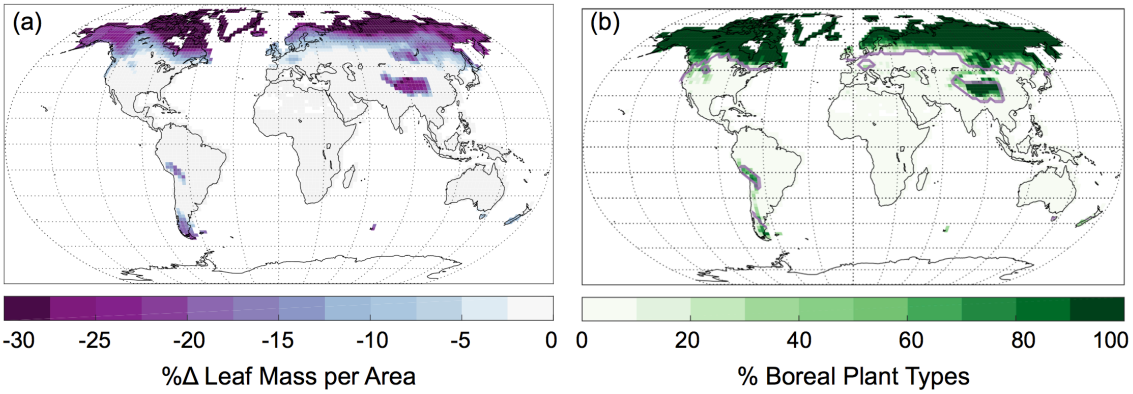

Figure S5. (a) Potential extent of leaf mass per area change (%) due to temperature acclimation estimated from growing season temperature change (CC - CTRL) and biome-specific acclimation relationships from Poorter et al. (2009). (b) Percent of simulated vegetated area covered by boreal plant types (boreal needleleaf evergreen and deciduous trees, boreal deciduous shrubs, and C_3 arctic grasses). Purple contours indicate -5% threshold for change in leaf mass per area due to temperature acclimation.

Table S1 List of Earth System Model Simulations

Name	[CO_2]	Δ LMA	Δ PS Rates	Description
CTRL	1xCO_2	-	-	*control*
LMA	1xCO_2	+1/3	-	*historical climate + leaf mass per area change*
CC	2xCO_2	-	-	*climate change only*
CCLMA	2xCO_2	+1/3	-	*climate change + upper range of leaf mass per area acclimation to CO_2*
CCLMAPS	2xCO_2	+1/3	+1/3	*climate change + upper range of leaf mass per area acclimation to CO_2 + greater photosynthetic rates*
TCCLMA	2xCO	+1/3, no Δ boreal & arctic	-	*climate change + upper range of leaf mass per area acclimation to CO_2 and temperature*

Note: [CO_2], prescribed atmospheric CO_2 concentration (1xCO_2 = 355ppm, 2xCO_2 = 710ppm); ΔLMA, prescribed change in leaf mass per area for C_3 plants; ΔPS Rates, prescribed change in maximum photosynthetic rates per area for C_3 plants.

Table S2 Confidence intervals for annual mean changes over land due to leaf trait acclimation (CCLMA - CC).

	Global		S. Extratropics		Tropics		N. Extratropics		N. High Latitudes	
	Mean	(95%CI)	Mean	(95%CI)	Mean	(95%CI)	Mean	(95%CI)	Mean	(95%CI)
Biogeophysical Warming (°C)	0.3	(0.2, 0.4)	0.3	(0.2, 0.4)	0.3	(0.2, 0.4)	0.4	(0.2, 0.5)	0.2	(0.0, 0.5)
Net primary productivity (PgC/yr)	-5.8	(-5.5, -6.0)	-0.8	(-0.7, -1.0)	-2.5	(-2.3, -2.8)	-2.1	(-1.9, -2.3)	-0.3	(-0.2, -0.3)
Leaf area index (m^2/m^2)	-0.9	(-0.9, -1.0)	-0.8	(-0.7, -0.8)	-1.0	(-1.0, -1.1)	-1.0	(-0.9, -1.0)	-0.6	(-0.5, -0.6)
Evapotranspiration (W/m^2)	-0.7	(-0.5, -0.9)	-0.9	(-0.2, -1.6)	-1.2	(-0.8, -1.5)	-0.4	(-0.1, -0.6)	-0.5	(-0.3, -0.7)
Transpiration (W/m^2)	-1.4	(-1.2, -1.5)	-1.9	(-1.4, -2.4)	-1.7	(-1.5, -1.9)	-1.1	(-1.0, -1.3)	-0.6	(-0.4, -0.7)
Leaf Evaporation (W/m^2)	-0.8	(-0.7, -0.8)	-0.7	(-0.5, -0.8)	-1.3	(-1.2, -1.5)	-0.5	(-0.5, -0.6)	-0.3	(-0.3, -0.4)
Soil Evaporation (W/m^2)	1.4	(1.3, 1.6)	1.6	(1.3, 1.9)	1.9	(1.8, 2.1)	1.3	(1.1, 1.4)	0.4	(0.3, 0.5)
Absorbed Solar Radiation (W/m^2)	0.6	(0.3, 0.8)	0.8	(0.1, 1.5)	0.6	(0.3, 1.0)	0.6	(0.3, 0.9)	-0.1	(-0.4, 0.2)